present as braids and irregular patches of fine dust). Moderate red to dark reddish-brown limonite is present as disseminations and irregular concentrational patches. Relatively coarse, interlocked sparry calcite grains are common as fracture/vein fillings.

1-2-3 Anjira Member

The Anjira Member is composed of interbedded limestone and shale. The limestone is thin bedded olive grey to olive black and weathers to yellowish brown. It is mainly allochemical packed to spare biomicritic. Some beds of pelmicritic limestone are also present. The shale is light olive grey and black, soft, friable and slightly non-calcareous.

1 − 3 Geological Structure

The geological structure generally trends north-south and forms the elevated hill in half the eastern area by anticline and the subsidence by syncline in the other half. In between the areas, the fault zone extends north-south.

Surmai-I : All the members of the Shirinab Formation are exposed. The Spingwar Member is exposed in the east, in fault contact with the Loralai Member. In the west, units of the Anjira Member are exposed. The area shows a broad anticline of which the eastern limb is faulted. The lower unit(No.1) shows extensive rolling and folding in the southeastern portion of the surveyed area. A major normal fault, striking north-south, is in the western part of the mapped area. The beds have been overturned and indicate a throw of about 200 metres. The dips are mostly 25° to 75°.

Surmai-II : The Unit IV of the Loralai and the two units of the Anjira are exposed. A north-south trending fault is present almost at the contact of the two units. The dips are gentle to high.

Srumai-III : All four units of the Loralai Member and the two units of the Anjira Member are exposed. The beds are steeply dipping and are folded. There are three major faults striking almost north-south in the area. One, in the west, dips west at an angle of 40-50° which truncates the western limb of the plunging anticline. The major fault in the centre, striking north-south, is a normal fault. The plane dips west and

the beds are displaced by about 100m. Another major fault striking north-south is at the eastern extremity of the mapped area. This is interpreted to be a reverse fault. The plane dips west and the beds are displaced by about 100 metres. Besides folding, the rolling of beds is also a common feature.

1－4 Mineralization

At Surmai,the mineralization is depicted by an oxidized outcrop (Gossan). The gossan is exposed as discoutinuous outcrops, outlining three different bodies: Surmai-Ⅰ, Ⅱ and Ⅲ.

Mineralization is in the form of veins along cross-cutting fractures, joints, bedding planes, and as partial replacement of limestone strata outward from fractures. The most distinctive characteristic of the surveyed area is its barite free zinc-lead mineralization as contrasted to the Gunga deposit. Ancient mining pits are present in the mineralized horizon, which may have been dug for lead. The gossan is composed of reddish brown, yellowish brown limonite, dark gray siderite, silicified and dolomitized limestone with veins filled in by dark brown limonites. Euhedral quartz crystals are common as cavity/vug fillings. Light yellowish spots, possibly of lead ochres, are common in the oxidized zone. Yellowish-greenish crustification, probably of smithsonite, also occurs. Massive galena contained in veins associated with limonite boxwork(Cellular type) having colloform texture together with euhedral to subhedral galena as disseminations,are common. Radiating aggregates of marcasite, partially to completely altered to limonite, have also been observed. Sideritization and silicification are possibly due to ore bearing solutions and were formed by metasomatic replacement of limestone.

1-4-1 Surmai Ⅰ

The main mineral indication is confined to near the boundary of UnitⅡ and Unit Ⅲ of the Loralai Member. It is 450m long and 60～80m wide, strikes N30°E, and dips 50～70°W as a strata-bound replacement conformable with host rocks.

1-4-2 Surmai II

The mineral indications are confined to Unit IV of the Loralai Member and Units I ~ II of the Anjira Member, they are composed of small scale gossans in the fault. They are the least important mineralizations, and it is presumed that the mineral indications present along the fault plane could be attributed to later mobilization due to tectonism.

1-4-3 Surmai III

The mineral indications are confined to Units II and III of the Loralai Member and are divided into two by location, the west mineral indication and the east mineral indication. Both of them are strata-bound replacements conformable with host rocks, partially associated with open-space fillings in solution collapsed breccia. The west mineral indication is some 1.5km long and 50~60m wide along the west limb of the north-south trending anticline, which plunges northward at a high angle. The east mineral indication is about 1.1 km long and 30~50m wide along the east limb of the east anticline which extends in a diretion parallel to the west anticline. Between both anticlines, mineral indications, west and east, may be identified below Quaternary debris which overlies synclinal host rocks.

Assay results of gossans are shown on Table II-1-2.

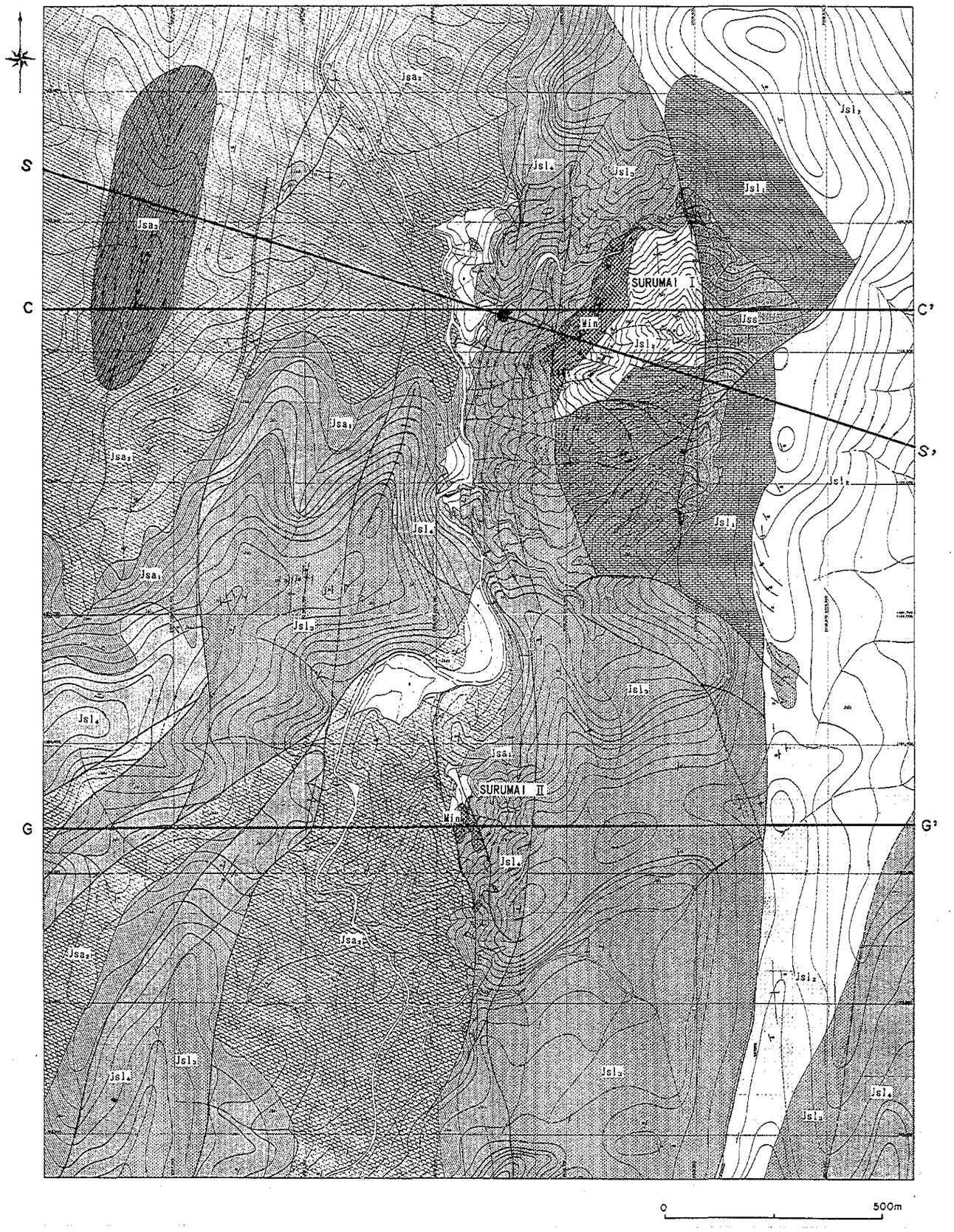

LEGEND

	Q	Alluvium	Dip(Normal)
	Jsa_3	Anjira member-Ⅲ	Dip(Overturned)
	Jsa_2	Anjira member-Ⅱ	Anticline
	Jsa_1	Anjira member-Ⅰ	Syncline
LOWER JURASSIC Shirinab Formation	Jsl_4	Loralai member-Ⅳ	Fault
	Jsl_3	Loralai member-Ⅲ	Bedding traces
	Jsl_2	Loralai member-Ⅱ	Profile line
	Jsl_1	Loralai member-Ⅰ	
	Jss	Spingwar member	Proposed drilling site
	Min	Mineralization	

Fig. Ⅲ-1-2 Geological Map of Surmai Area(Surmai-Ⅰ, Ⅱ)

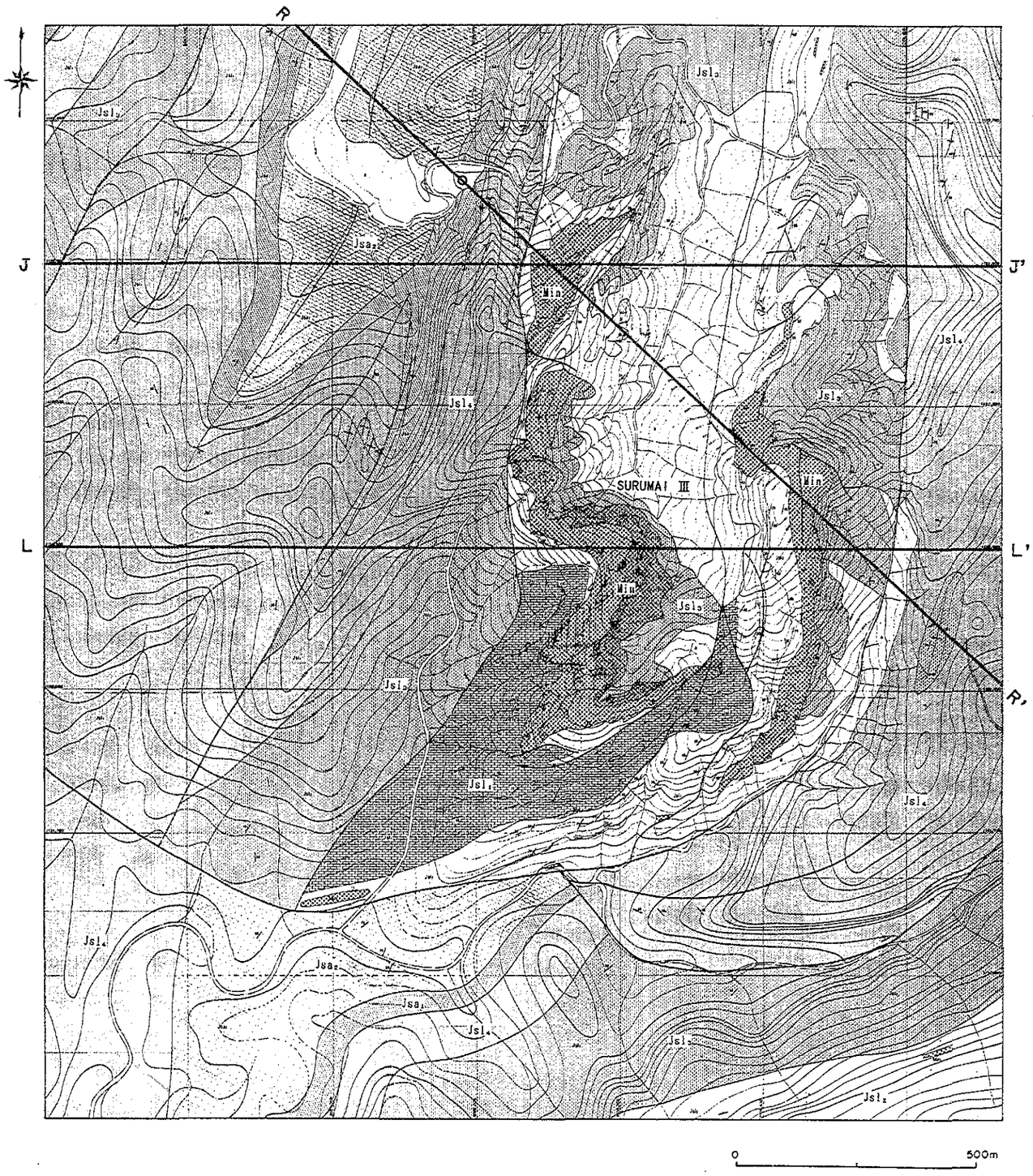

LEGEND

	Q	Alluvium	Dip(Normal)
	Jsa_3	Anjira member-Ⅲ	Dip(Overturned)
	Jsa_2	Anjira member-Ⅱ	Anticline
	Jsa_1	Anjira member-Ⅰ	Syncline
LOWER JURASSIC	Jsl_4	Loralai member-Ⅳ	Fault
Shirinab Formation	Jsl_3	Loralai member-Ⅲ	Bedding traces
	Jsl_2	Loralai member-Ⅱ	Profile line
	Jsl_1	Loralai member-Ⅰ	
	Jss	Spingwar member	Proposed drilling site
	Min	Mineralization	

Fig. Ⅲ-1-3 Geological Map of Surmai Area(Surmai-Ⅲ)

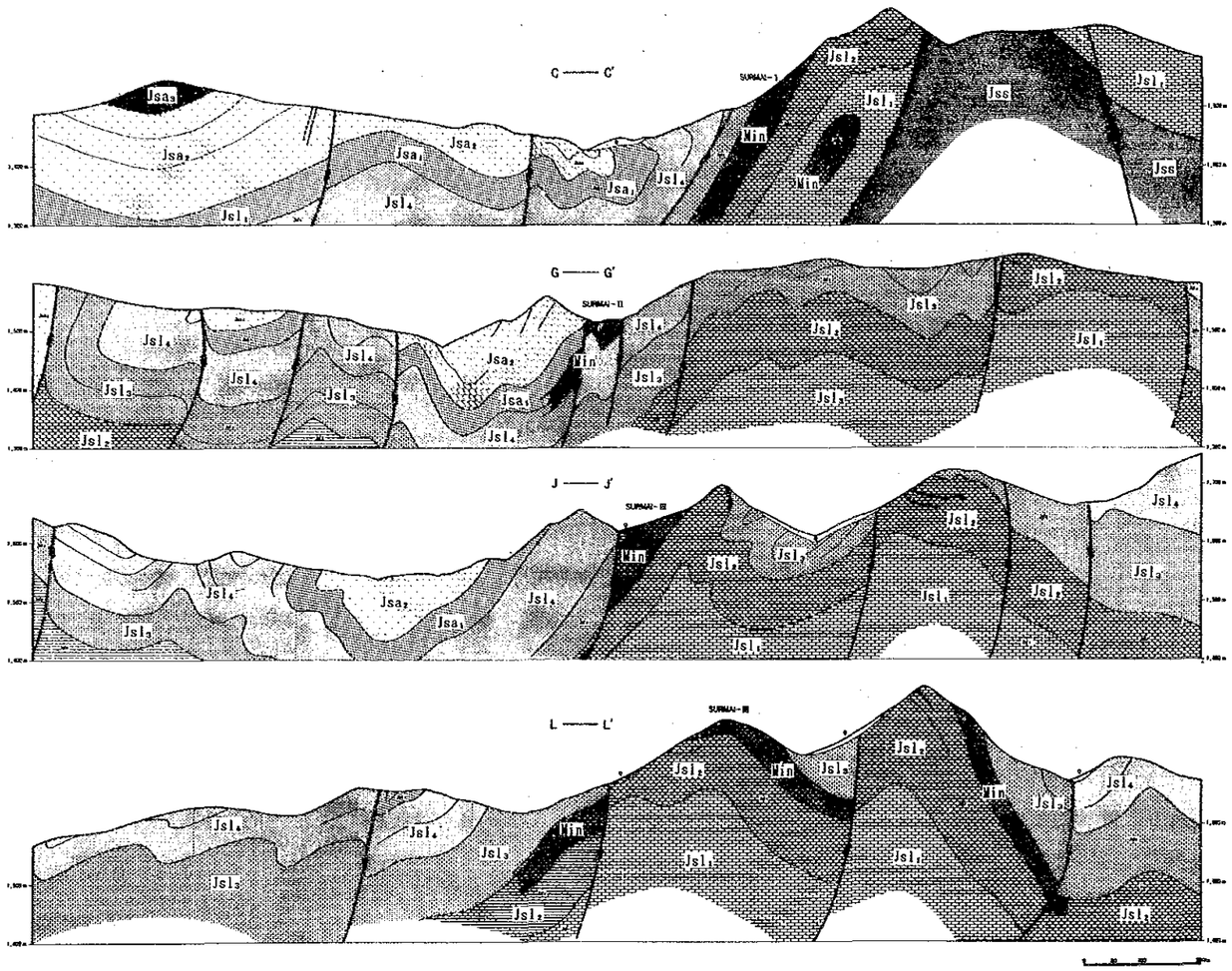

LEGEND

	Q	Alluvium
	Jsa_3	Anjira member-Ⅲ
	Jsa_2	Anjira member-Ⅱ
	Jsa_1	Anjira member-Ⅰ
LOWER JURASSIC Shirinab Formation	Jsl_4	Loralai member-Ⅳ
	Jsl_3	Loralai member-Ⅲ
	Jsl_2	Loralai member-Ⅱ
	Jsl_1	Loralai member-Ⅰ
	Jss	Spingwar member
	Min	Mineralization
	——	Fault
	----	Bedding traces
	A——A'	Profile line

Fig. Ⅲ-1-4 Geological Profiles of Surmai Area

Chapter 2 Geochemical survey

2－1 Outline

A rock geochemical survey was conducted in the Surmai Area. The rock types for the survey were mainly carbonate rocks of the Shirinab Formation and gossans which occurred in the Loralai Member. A total of 205 samples were collected - 36 from the gossans, 3 from the Spingwar Member, 18 from Loralai Unit Ⅰ, 31 from Loralai Unit Ⅱ, 44 from Loralai Unit Ⅲ, 34 from Loralai Unit Ⅳ, 12 from Anjira Unit Ⅰ, 25 from Anjira Unit Ⅱ and 2 from Anjira Unit Ⅲ. All of the samples were pulverized to under 80 mesh size. A nitric-aqua regia method was used for digestion of these pulverized samples. Six elements, Pb, Zn, Ba, Mg, Hg and S, were analyzed by atomic absorption spectrophotometry(AAS).

2－2 Statistical Treatment of Geochemical Analyses Data

The cumulative frequency distributions of 6 elements (Pb, Zn,Hg, Ba, Mg and S) are shown in Fig.Ⅲ-2-2. The threshold, the upper limit of local background, for each element was determined with reference to Sinclair(1976) as below. Abbreviations of statistical terms are as follows. Th:Threshold, M:mean, σ :standard deviation, n: number of sample, and γ :correlation coefficient.

Table Ⅲ-2-1 Threshold Value of Surmai Area(n:205)

	Pb ppm	Zn ppm	Hg ppm	Ba ppm	Mg ppm	S %
Threshold	2,000	1,000	750	420	10,500	0.05

Table Ⅲ-2-2 Threshold Value of Surmai Area(n:169)

(excluded 36 samples at gossans)

	Pb ppm	Zn ppm	Hg ppm	Ba ppm	Mg ppm	S %
Threshold	350	700	500	290	8,000	0.039

The frequency distribution (histgram) of 6 elements in 205 samples are shown in Fig.Ⅲ-2-1.

The statistical parameters, means, and standard deviations etc. of the 205 samples stratified according to Members and gossans, are given in TableⅢ-2-3.

The scatter diagrams and correlation coefficients for each pair of

variables(Pb,Zn,Hg,Ba,Mg and S) are given, respectively, in FigⅢ-2-3 and TableⅢ-2-6.

TableⅢ-2-3 List of Statistic Parameters in Surmai Area (n:205)

Numbers	Mean(M)	Min.Value	Max.Value	σ	M+σ	M+2σ
Pb (ppm)	26.70	1	10,000	1.173	397	5,913
Zn (ppm)	133.40	9	10,000	0.845	933	6,529
Hg (ppb)	64.40	10	40,000	0.795	401	2,505
Ba (ppm)	230.64	50	1,620	0.244	357	627
Mg (ppm)	4,384	600	61,000	0.290	8,546	16,659
S (%)	0.632	<0.001	<0.001	0.632	0.015	0.063

σ : log.

2－3 Analytical Results

2-3-1 Distribution of Elements in Jurassic Members

The average abundance of the 6 elements in igneuos rocks, sandstones, shales, and limestones forms the basis for establishing background for these elements(TableⅢ-2-5).

TableⅢ-2-5 Average Content of 6 Elements in Seddimentary Rocks and Igneous Rocks

Element	Igneous rocks	Sandstones	Shales	Limestone
Mg	20,900	7,100	14,800	47,700
S	520	2,800	2,600	1,100
Zn	132	20	200-1,000	50
Ba	250	170	460	120
Hg	0.077-0.5	0.1	0.3	0.03
Pb	16	20	20	5.10

(Elements given in g/ton, source:Rankama and Sahama,1950)

TableⅢ-2-3, above, shows that only the Mg content in the Jurassic members is low compared with average element contents in limestone of Table.

(1) Lead : Lead has a strong tendency to statistically be distributed in concentration in Loralai Units Ⅰ,Ⅱ and Ⅲ. The test of the difference of the mean values between Loralai Units Ⅰ, Ⅱ and Ⅲ, and other members presents a statisitical significance. The surface distribution of Pb in rocks and gossans is shown in Fig.Ⅲ-2-4. The high concentrations of Pb

naturally occur in the gossans, Surmai Ⅰ, Ⅱ and Ⅲ, and it decreases in content toward non-mineralized rocks.

(2) Zinc : As Fig.Ⅲ-2-5 shows, the distribution of Zn in exposed rocks and gossans has a similar pattern as that of Pb. The geometric mean value of Zn content in Loralai Units Ⅰ, Ⅱ and Ⅲ combined is approximately twice those of Anjira and Loralai Unit Ⅳ, and 3 times as that of Spingwar (TableⅢ-2-1). The highest concentration of Zn occurs in the gossan of Surmai Ⅲ, and zinc shows a pronounced tendency to decrease in concentration towards unmineralized carbonate rocks.

(3) Mercury : The high concentrations of Hg(more than 499,490.5 ppm=M+3σ, n=36 at the gossans) occur in the gossans of Surmai Ⅰ, Ⅱ and Ⅲ. Fig.Ⅲ-2-6 shows that the distribution of Hg in rocks and gossans has a similar pattern as those of Pb and Zn. The geometric mean value of Hg content of the combined Loralai Units Ⅰ, Ⅱ and Ⅲ is higher than that of other units.

(4) Barium : The high concentrations of Ba (more than 630 ppm≒M+2σ, n=205) occur in the carbonate rocks of the Loralai Member near the contact with the Surmai Ⅲ gossan in the north and the Surmai Ⅰ gossan in the south. The geometric mean of Ba content of each Unit and the gossans range in weight ratio from 123 ppm at minimum value in the gossans to 243 ppm at maximum value in the Anjira. The surface distribution of Ba in rocks and gossans is shown in FigⅢ-2-7. Barium concentrations greater than the mean value at the limit of sampling lie in carbonate rocks of the Loralai and Anjira,not in the gossans.

(5) Magnesium : The anomalies of Mg concentration(more than 10,500 ppm≒Th) lie in carbonate rocks of the Anjira and the Loralai, and in the sandstone of the Spingwar. The geometric mean of Mg content of each unit and of the gossans range in weight ratio from 3,255 ppm at minimum value in the gossans to 5,646 ppm at maximum in the Spingwar. The distribution of Mg as well as Ba shows a pronounced negative anomaly over the gossans (FigⅢ-2-8).

(6) Sulpher : The high concentrations of S occur in the gossans. The geometric mean of S content of each Unit and of the gossans range in percentage from 0.002% at minimum in Loralai Ⅰ, Ⅱ and Ⅲ, and the Spingwar to 0.009% at maximum in the gossans. As FigⅢ-2-9 shows, S generally increases in concentration towards the gossans, especially in Surmai Ⅰ and Ⅱ.

2-3-2 Relationships among Elements

Correlation coefficient between the elements for all samples in the Surmai area is shown in TableⅢ-2-6.

TableⅢ-2-6 Coefficiency of Correlation of 6 Elements in Surmai Area

	Pb				
Zn	0.901	Zn			
Ba	-0.417	-0.453	Ba		
Mg	-0.176	-0.238	0.183	Mg	
Hg	0.812	0.838	-0.393	-0.244	Hg
S	0.175	0.165	0.163	-0.027	0.287

The high correlation is observed between Pb and Zn Hg,Zn and Hg.

2-3-3 Extraction and Evaluation of Anomalous Areas

The mineralized zone,the gossan on surface is characterized by the high content of Pb, Zn, and Hg, and the low content of Ba and Mg in comparison with non-mineralized rocks. Anomaly of Ba has a tendency to lie on hanging wall or foot wall of the gossans. Considering those peculiarities in distribution of elements, two anomalous areas are extracted as follows.

① The area between Surmai Ⅱ and Surmai Ⅲ; Approximately 1.0 km north-south extention with 300 m wide shows a weak anomaly in Pb, Zn, and Hg.

② The south-westward area of Surmai Ⅱ; Approximately 800 m northeast-southwest trend with 300 m wide also shows a weak anomaly in Pb, Zn, and Hg.

Evaluation on ① and ② are as follows.

① It shows the possibility of emplacement of mineral indications that would be northward extention of Surmai Ⅲ.

② No development of mineral indications are expected due to geological structure on the area.

Table Ⅲ-2-4 List of Statistic Parameters in Member of shirinab Formation, Surmai Area

Elements \ Group		Total	Anjira Member	Loralai Member			Spingwar Member	Mineralized Zone
				Ⅰ, Ⅱ, Ⅲ	Ⅳ	total		
	N	169 *	39	93	34	127	3	36
Pb	min	1	1	1	1	1	9	4
	max	900	68	900	430	900	74	10,000
	σ	0.781	0.629	0.795	0.797	0.811	0.374	1.050
	平均(M)	11.12	6.08	16.34	7.23	13.14	25.19	1,626
	M+σ	67	25	101	45	85	59	18,241
	M+2σ	406	110	636	284	550	140	204,549
	M+3σ	2,454	470	3,972	1,782	3,562	333	2,293,713
Zn	min	9	12	13	9	9	20	19
	max	8,630	490	8,630	1,080	8,630	44	10,000
	σ	0.519	0.326	0.568	0.47	0.558	0.147	0.861
	平均(M)	70.42	48.13	96.21	49.78	80.63	31.93	2,676
	M+σ	232	101	355	146	291	44	19,415
	M+2σ	770	215	1,317	431	1,053	62	140,845
	M+3σ	2,546	456	4,873	1,268	3,805	88	1,021,752
Hg	min	10	10	10	10	10	20	20
	max	4,000	4,000	1,500	260	1,500	30	29,000
	σ	0.477	0.597	0.438	0.372	0.438	0.08	0.899
	平均(M)	35.90	37.69	35.74	42.28	22.58	22.89	1,000
	M+σ	107	149	115	53	98	27	7,939
	M+2σ	322	589	317	125	269	33	62,972
	M+3σ	969	2,332	871	295	738	40.62	499,490
Ba	min	100	160	120	100	100	180	50
	max	1,400	980	1,400	1,240	1,400	220	1,620
	σ	0.200	0.185	0.203	0.213	0.206	0.037	0.307
	平均(M)	226.67	243.16	222.53	222.82	222.60	195.95	123.14
	M+σ	359	372	354	364	357	213	249
	M+2σ	569	569	565	595	569	232	509
	M+3σ	902	872	902	974	921	253	1,030
Mg	min	600	2,200	1,700	1,200	1,200	600	1,050
	max	38,500	16,000	38,500	35,500	38,500	20,000	61,000
	σ	0.279	0.173	0.294	0.267	0.288	0.690	0.304
	平均(M)	4,671	4,520	4,849	4,306	4,698	5,646	3,255
	M+σ	8,882	6,725	9,547	7,965	9,120	27,674	6,559
	M+2σ	16,888	10,005	17,706	18,796	14,735	135,649	13,219
	M+3σ	32,112	14,887	39,003	27,257	34,374	664,884	26,641
S	min	<0.001	<0.001	<0.001	<0.001	<0.001	<0.001	<0.001
	max	0.04	0.025	0.04	0.02	0.004	0.005	1.21
	σ	0.553	0.535	0.545	0.563	0.554	0.429	0.793
	平均(M)	0.003	0.0039	0.002	0.003	0.003	0.002	0.009
	M+σ	0.009	0.013	0.008	0.011	0.009	0.005	0.056
	M+2σ	0.036	0.046	0.029	0.044	0.033	0.014	0.344
	M+3σ	0.128	0.157	0.100	0.159	0.116	0.038	2.135

* N : Number of Samples except mineralized zone

σ : log.

Table Ⅲ-2-7 Coefficiency of Correlation of 6 Elements for Member of Shirinab Formation in Surmai Area

Total (N:169)

	Pb	Zn	Ba	Mg	Hg
Zn	0.760				
Ba	-0.058	-0.089			
Mg	-0.010	-0.128	0.040		
Hg	0.564	0.598	-0.019	-0.080	
S	-0.088	-0.083	0.296	0.085	0.072

Anjira M - II

	Pb	Zn	Ba	Mg	Hg
Zn	0.617				
Ba	-0.256	-0.148			
Mg	0.215	0.180	-0.187		
Hg	0.335	0.381	-0.075	-0.146	
S	-0.066	0.049	0.243	-0.210	0.249

Loralai M - IV

	Pb	Zn	Ba	Mg	Hg
Zn	0.717				
Ba	0.152	0.027			
Mg	-0.217	-0.296	0.061		
Hg	0.772	0.527	0.257	-0.223	
S	-0.061	-0.074	0.096	-0.012	0.137

Lorlai M - III

	Pb	Zn	Ba	Mg	Hg
Zn	0.863				
Ba	-0.119	-0.069			
Mg	0.031	-0.088	0.097		
Hg	0.769	0.704	-0.126	0.009	
S	-0.197	-0.150	0.406	0.320	-0.141

Loralai M - II

	Pb	Zn	Ba	Mg	Hg
Zn	0.741				
Ba	-0.063	-0.190			
Mg	0.158	-0.146	0.125		
Hg	0.674	0.813	-0.148	-0.032	
S	0.078	0.068	0.544	0.257	0.131

Loralai - I

	Pb	Zn	Ba	Mg	Hg
Zn	0.817				
Ba	0.076	0.057			
Mg	-0.280	-0.249	-0.148		
Hg	0.576	0.684	0.112	-0.050	
S	0.179	-0.014	0.240	-0.255	0.168

Spingwa M

	Pb	Zn	Ba	Mg	Hg
Zn	0.715				
Ba	0.222	0.840			
Mg	-0.848	-0.237	0.328		
Hg	0.885	0.308	-0.257	-0.997	
S	-0.767	-0.100	0.456	0.990	-0.977

Total (N:36)

	Pb	Zn	Ba	Mg	Hg
Zn	0.904				
Ba	-0.513	-0.547			
Mg	-0.161	-0.154	0.309		
Hg	0.752	0.812	-0.405	-0.306	
S	0.021	-0.067	0.410	-0.104	0.182

Correlation Diagram of Mineralized Area

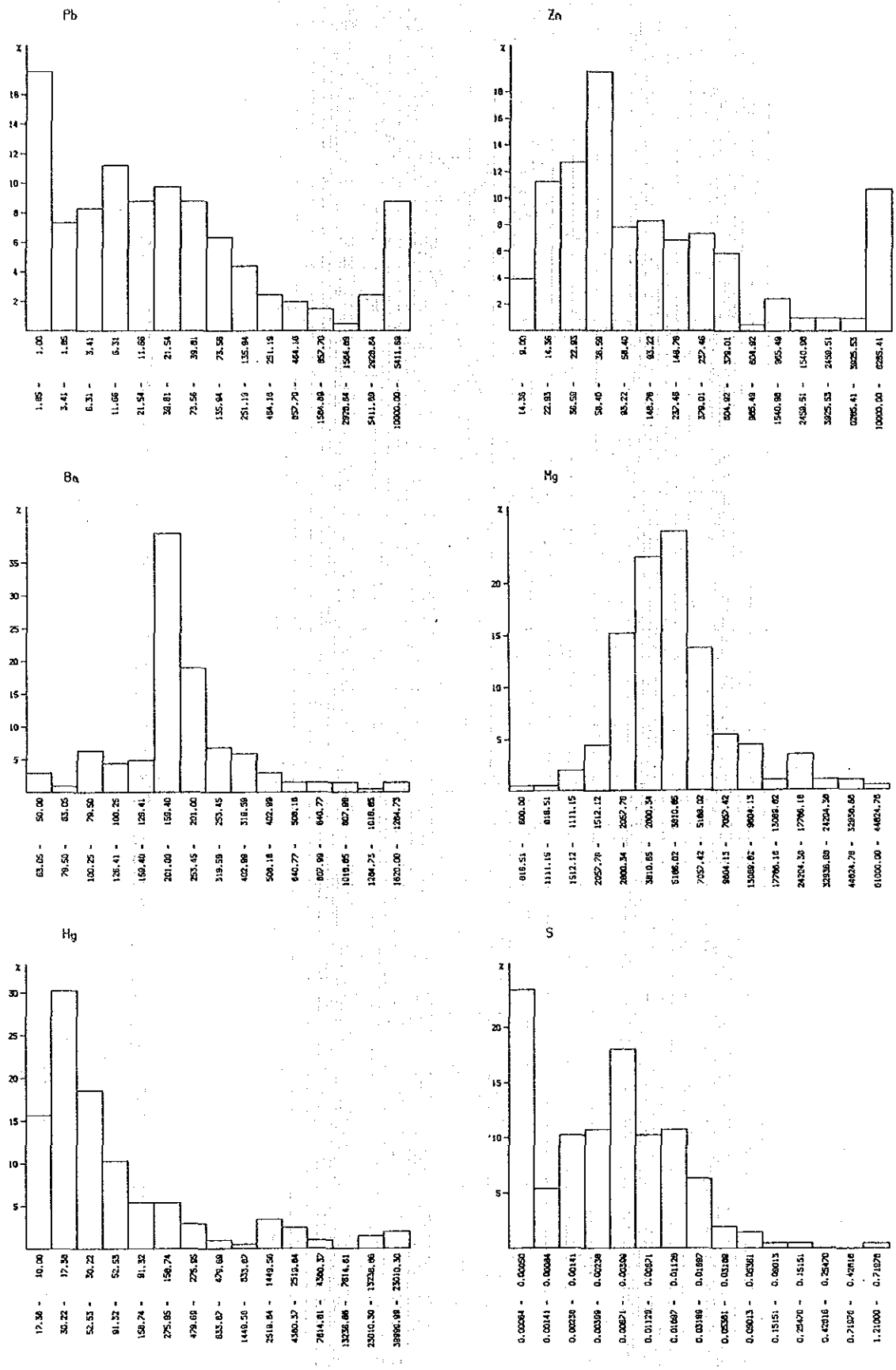

Fig. Ⅲ-2-1 Histogram of 6 Elements in Surmai Area

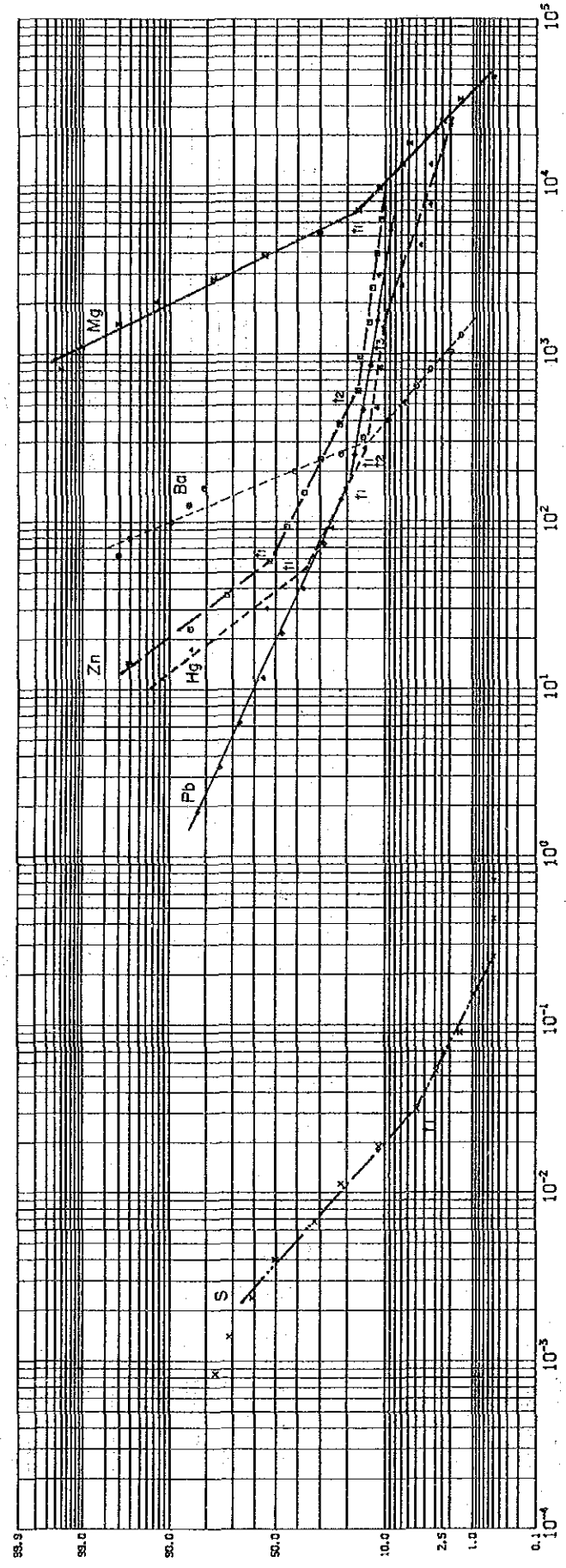

Fig. Ⅲ-2-2 Cumulative Frequency Distribution Curve of 6 Elements in Surmai Area

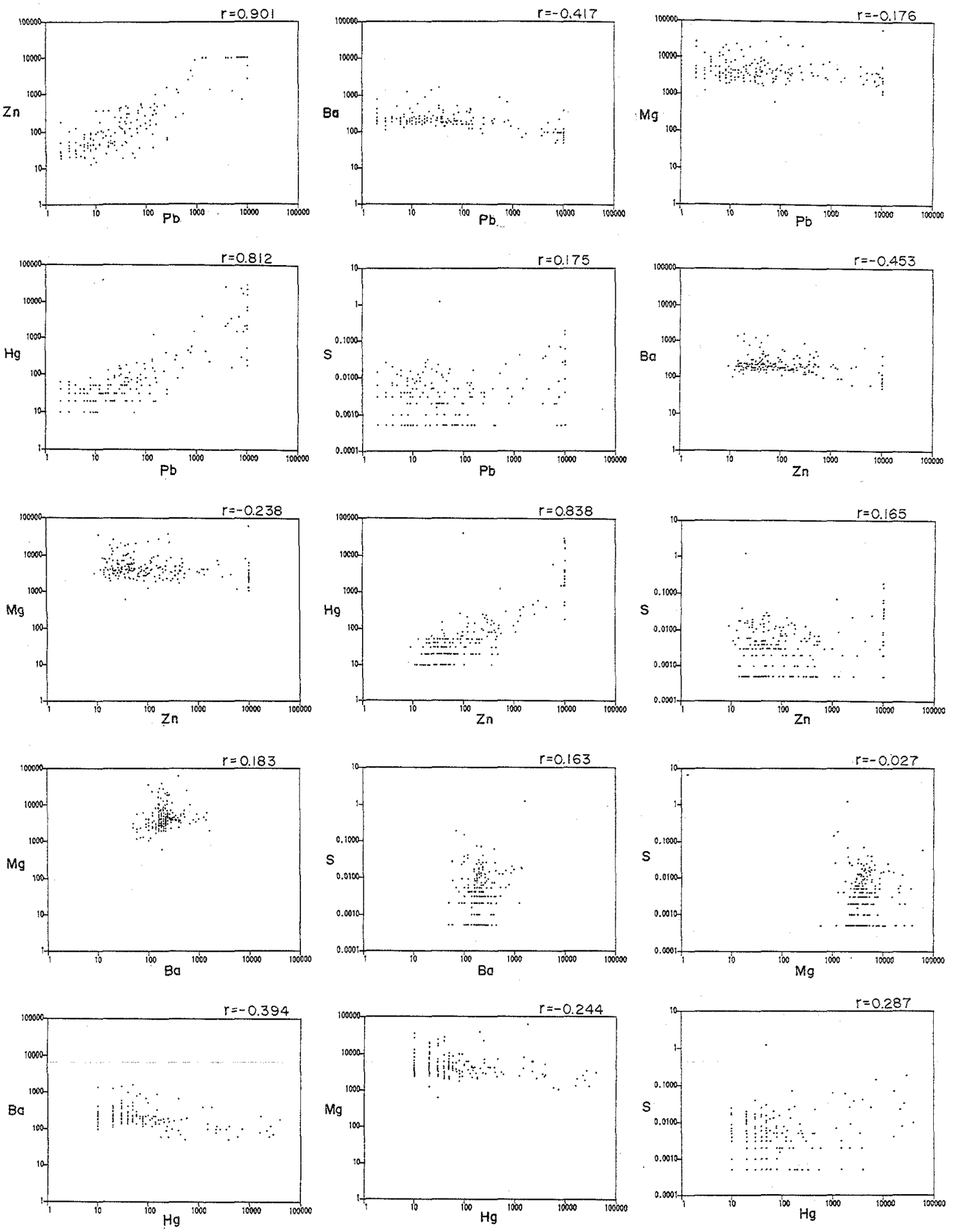

r = Coefficient of Correlation

Fig. Ⅲ-2-3 Correlation Diagram of 6 Elements in Surmai Area

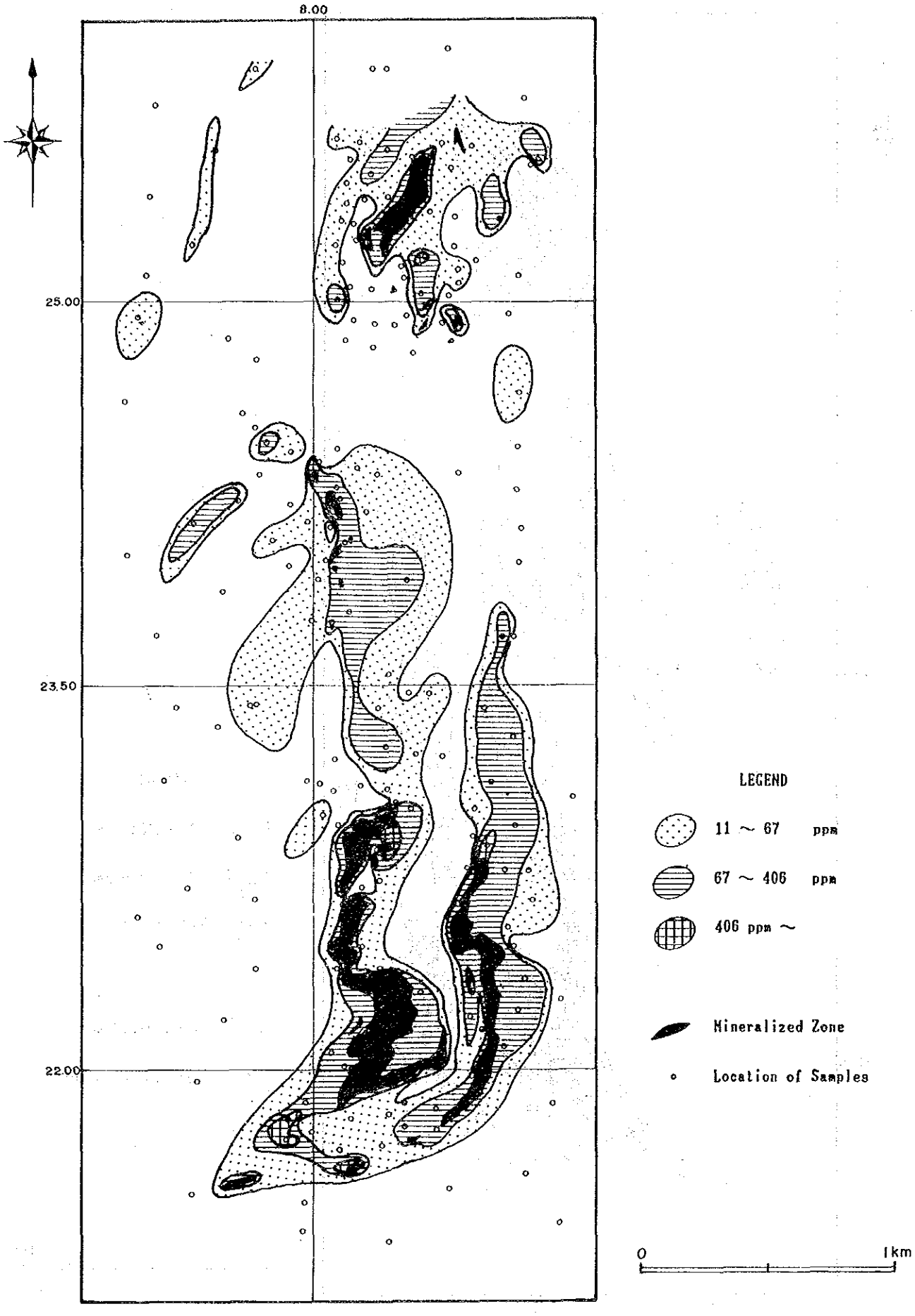

Fig. Ⅲ-2-4 Distribution of Lead in Surmai Area

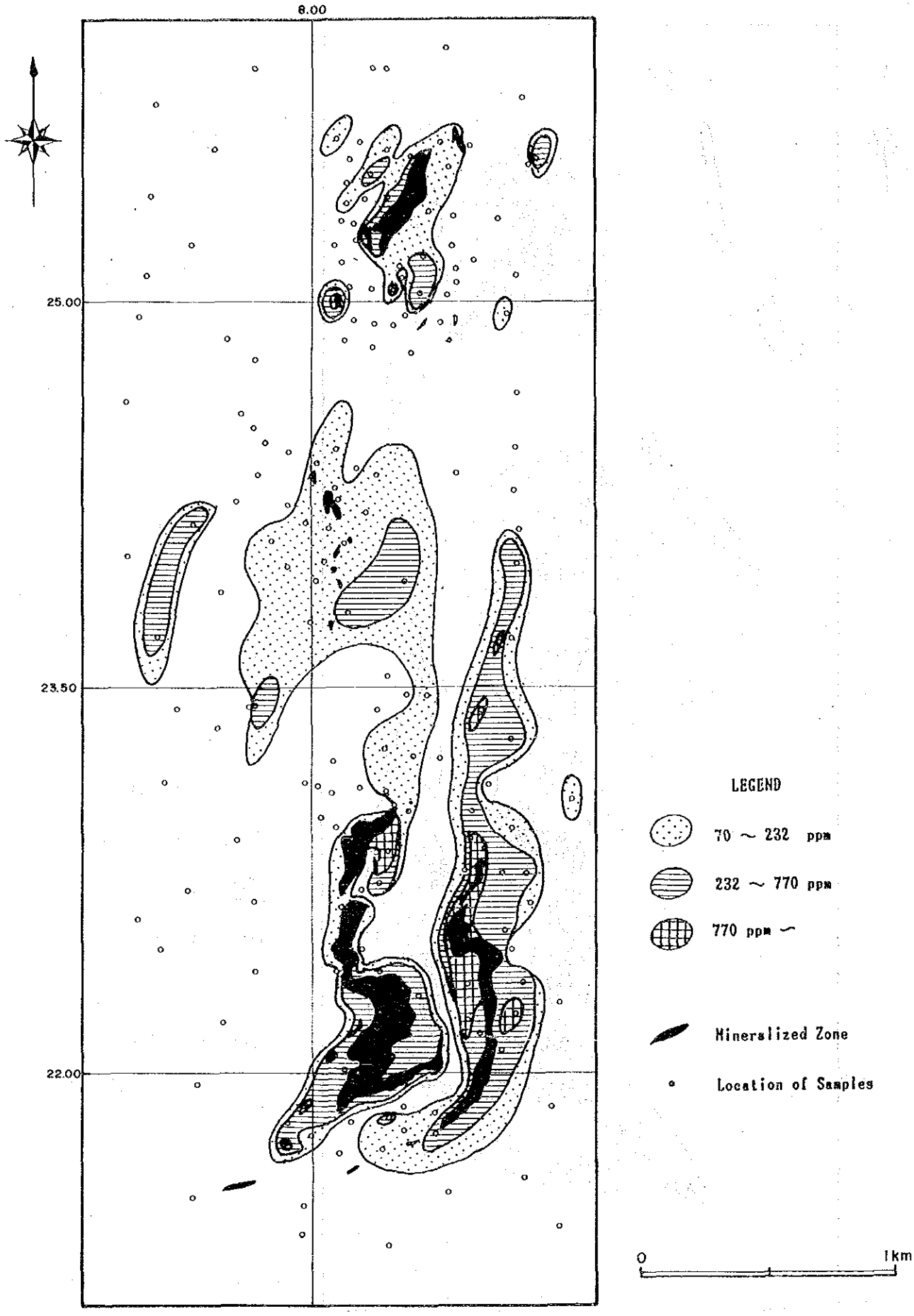

Fig. Ⅲ-2-5 Distribution of Zinc in Surmai Area

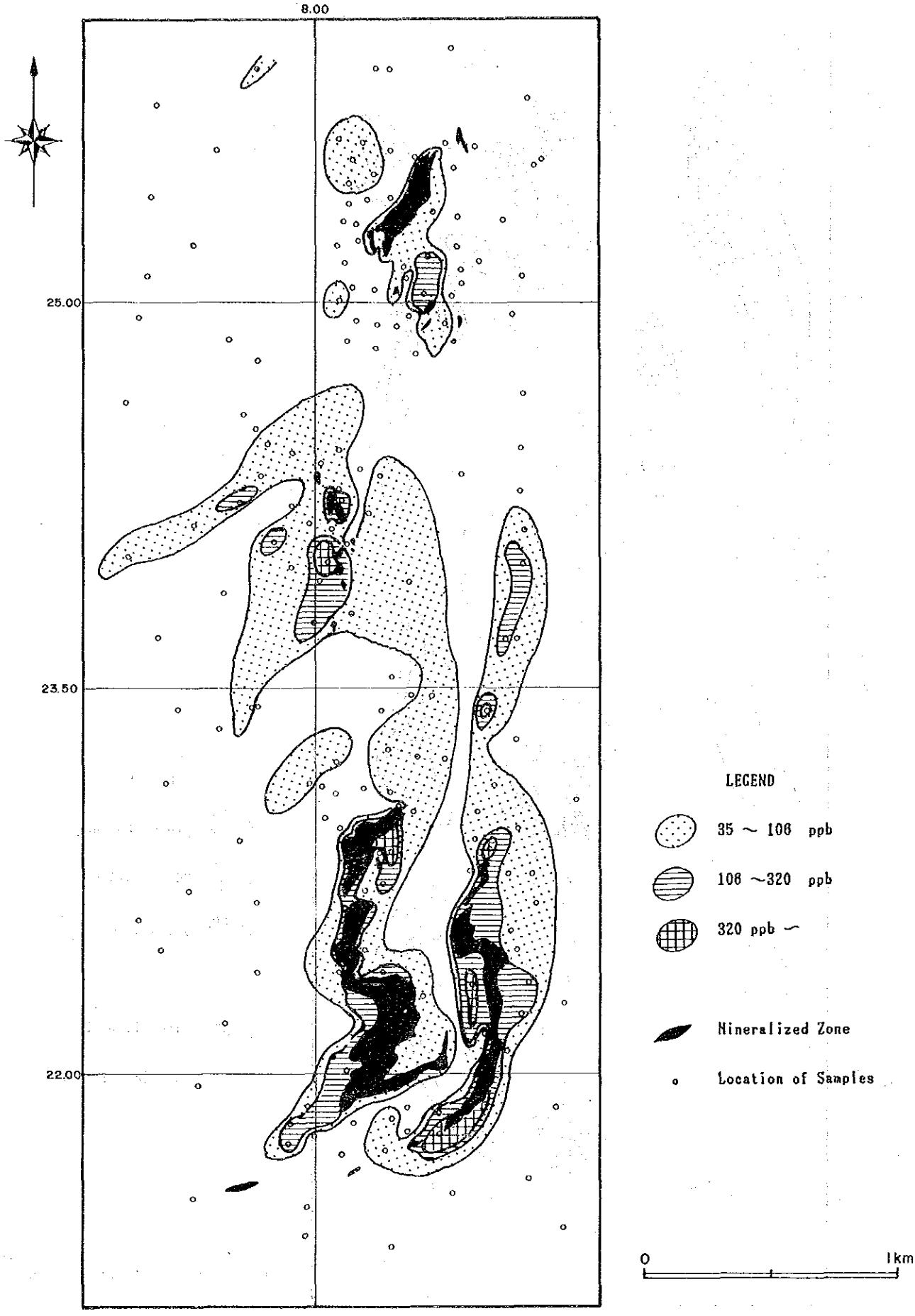

Fig. Ⅲ-2-6 Distribution of Mercury in Surmai Area

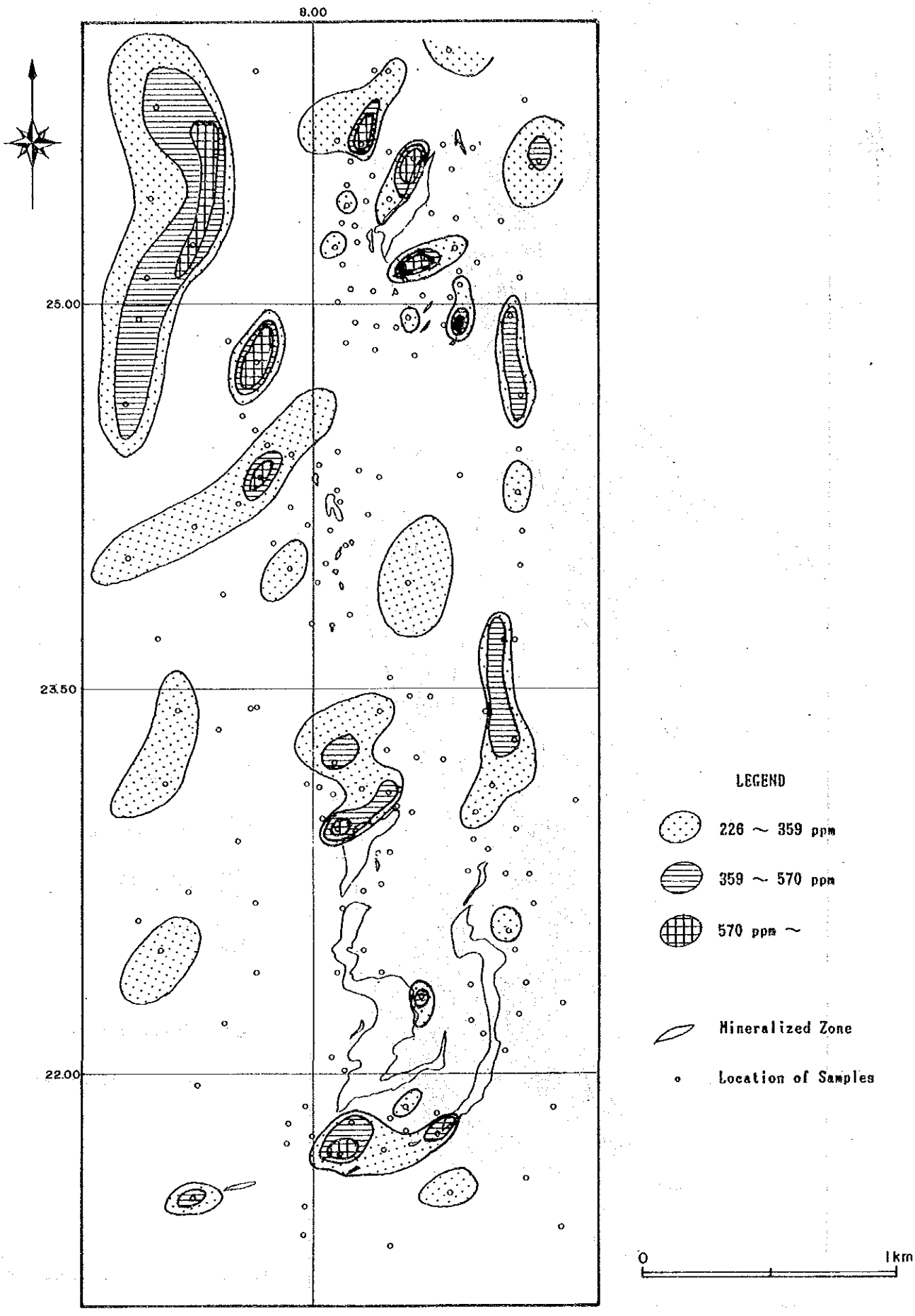

Fig. Ⅲ-2-7 Distribution of Barium in Surmai Area

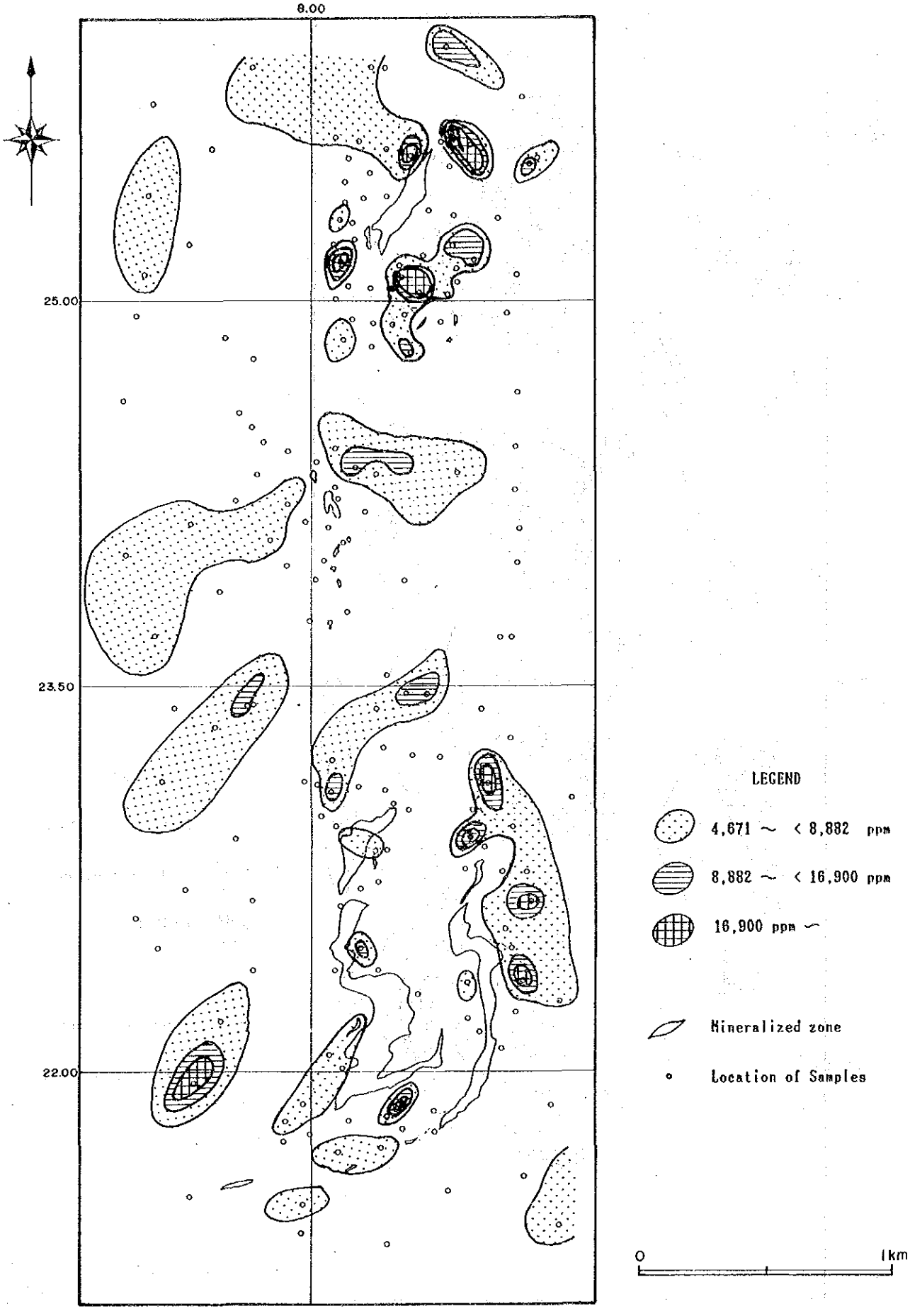

Fig. Ⅲ-2-8 Distribution of Magnesium in Surmai Area

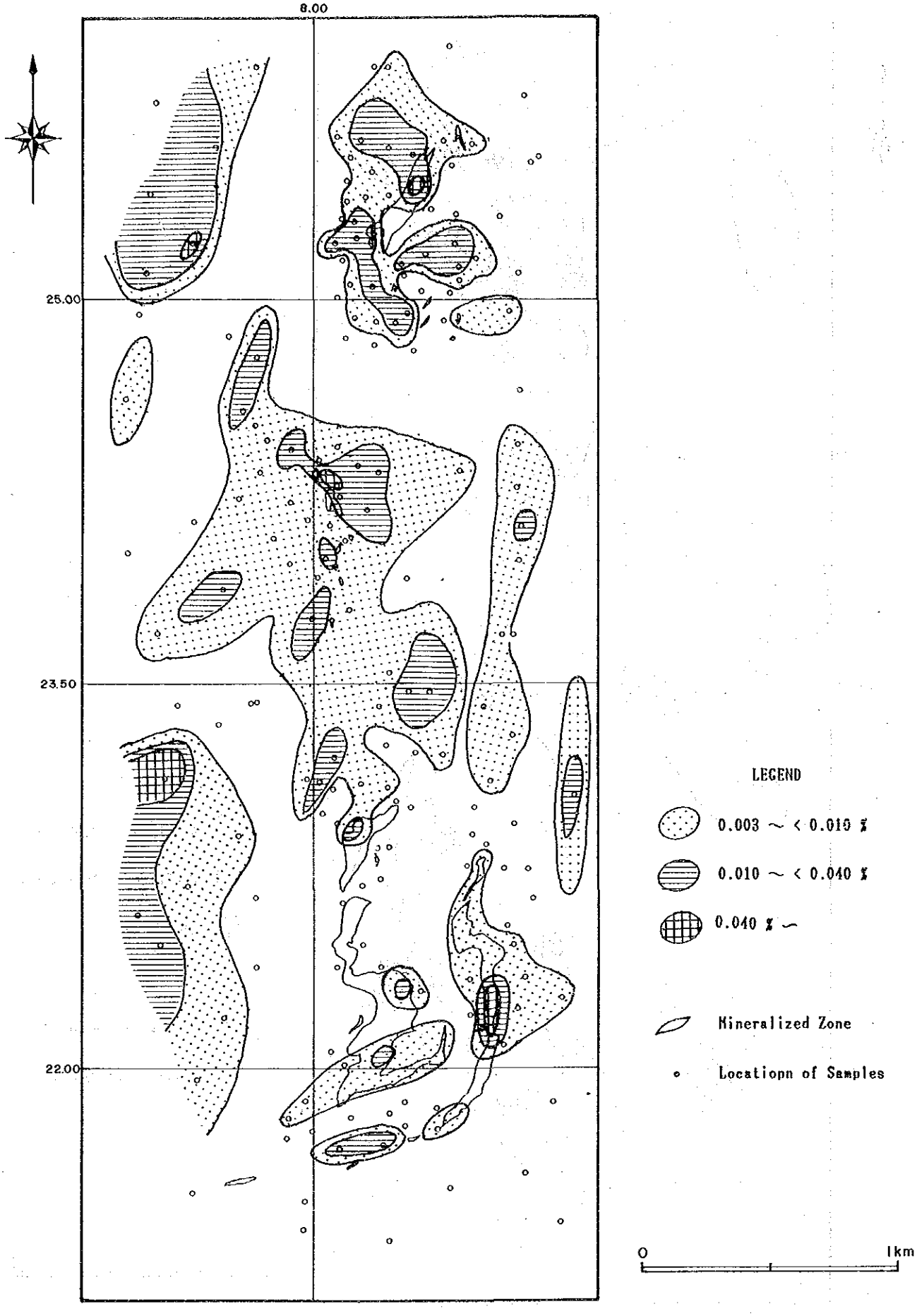

Fig. Ⅲ-2-9 Distribution of Sulphur in Surmai Area

Chapter 3 Geophysical Survey (SIP & IP Methods)

3-1 Outline of the Survey

3-1-1 Survey Area

Two areas, the Surmai and Gunga Mine areas, as shown in Fig. Ⅰ-1-1 were investigated with geophysical methods (SIP and IP).

The Surmai area is located about 13 km southwest of Khuzdar and 7 km southeast of Gunga Village. The three mineralized parts are called Surmai Ⅰ, Ⅱ and Ⅲ from north to south. The arrangement of survey lines in those areas is illustrated in Figs. Ⅲ-3-1～Ⅲ-3-3 respectively.

The Gunga Mine area is located about 3 km SSE of Gunga Village and about 2 km north of Surmai Ⅰ. It is accessible in about 25 minuites from Khuzdar by jeep. The arrangement of survey lines in the Gunga Mine area is illustrated in Fig. Ⅲ-3-4.

3-1-2 Survey Specifications

Field work specifications were set as follows :

a. Length of Survey Line 17.2 km in twenty lines
   SIP 9.4 km in eleven lines 490 points
   I P 7.8 km in nine lines 420 points
   Length and measurement points for each line are shown in Table Ⅲ-3-1.

b. Survey Line Separation : Surmai Ⅰ, Ⅱ 150 m
   Surmai Ⅲ 300 m
   Gunga Mine 240 m

c. Electrode Configuration : dipole-dipole array

d. Electrode Separation : Surmai Ⅰ, Ⅱ and Gunga Mine a= 50 m
   Surmai Ⅲ a=100 m

e. Electrode Separation coefficient : n = 1 ～ 5

f. Measurement Method : Frequency domain

g. Frequencies : SIP 0.125 ～ 88 Hz (18 frequencies)
   I P 0.3 / 3.0 Hz

3-1-3 Survey Method

SIP is the abbreviated form of spectral induced polarization and the method operates on the same principle as the conventional IP method. The SIP

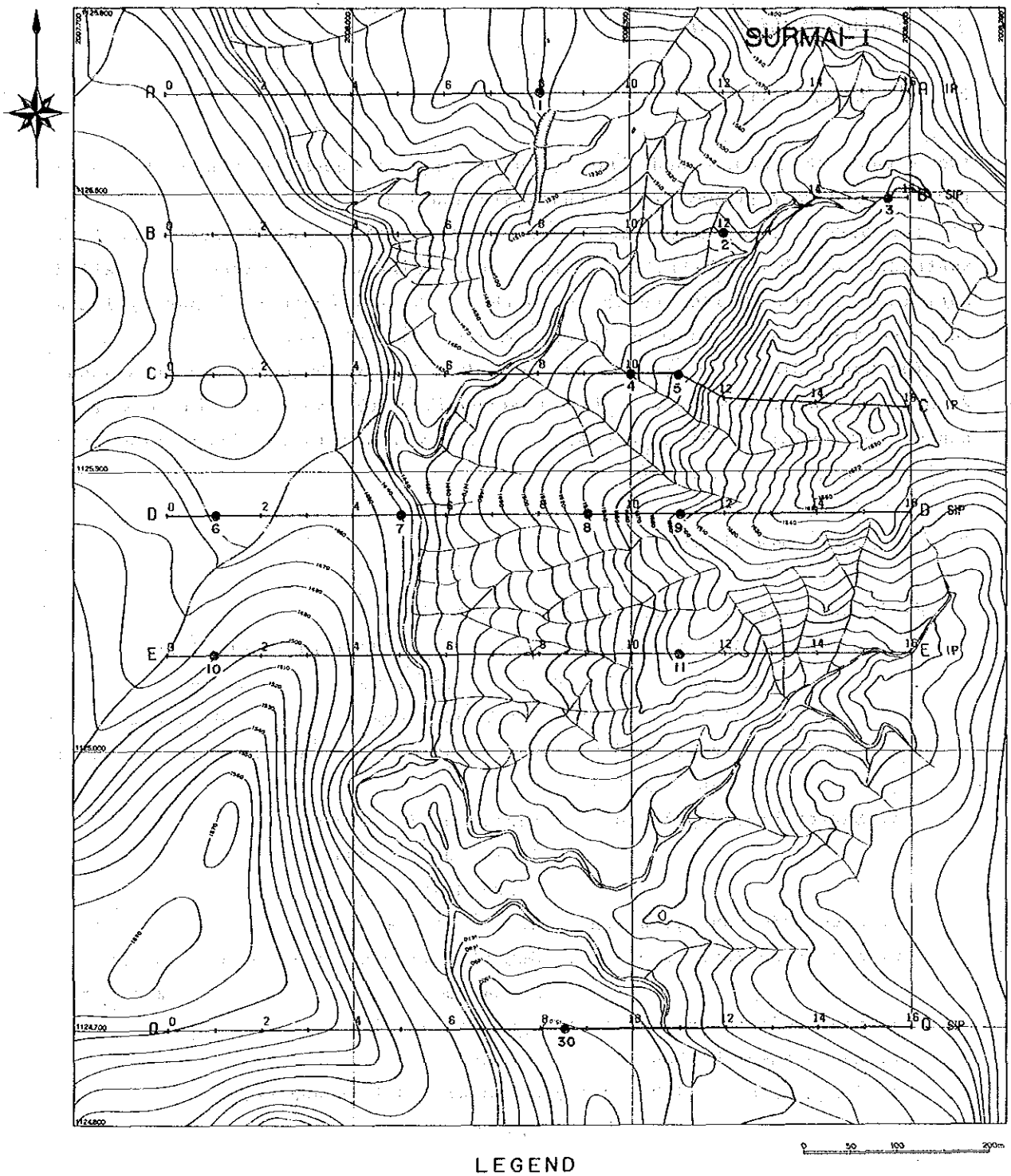

LEGEND

12 Location of Rock Samples

Survey Line

Fig. Ⅲ-3-1 Location Map of Survey Lines in Surmai I Area

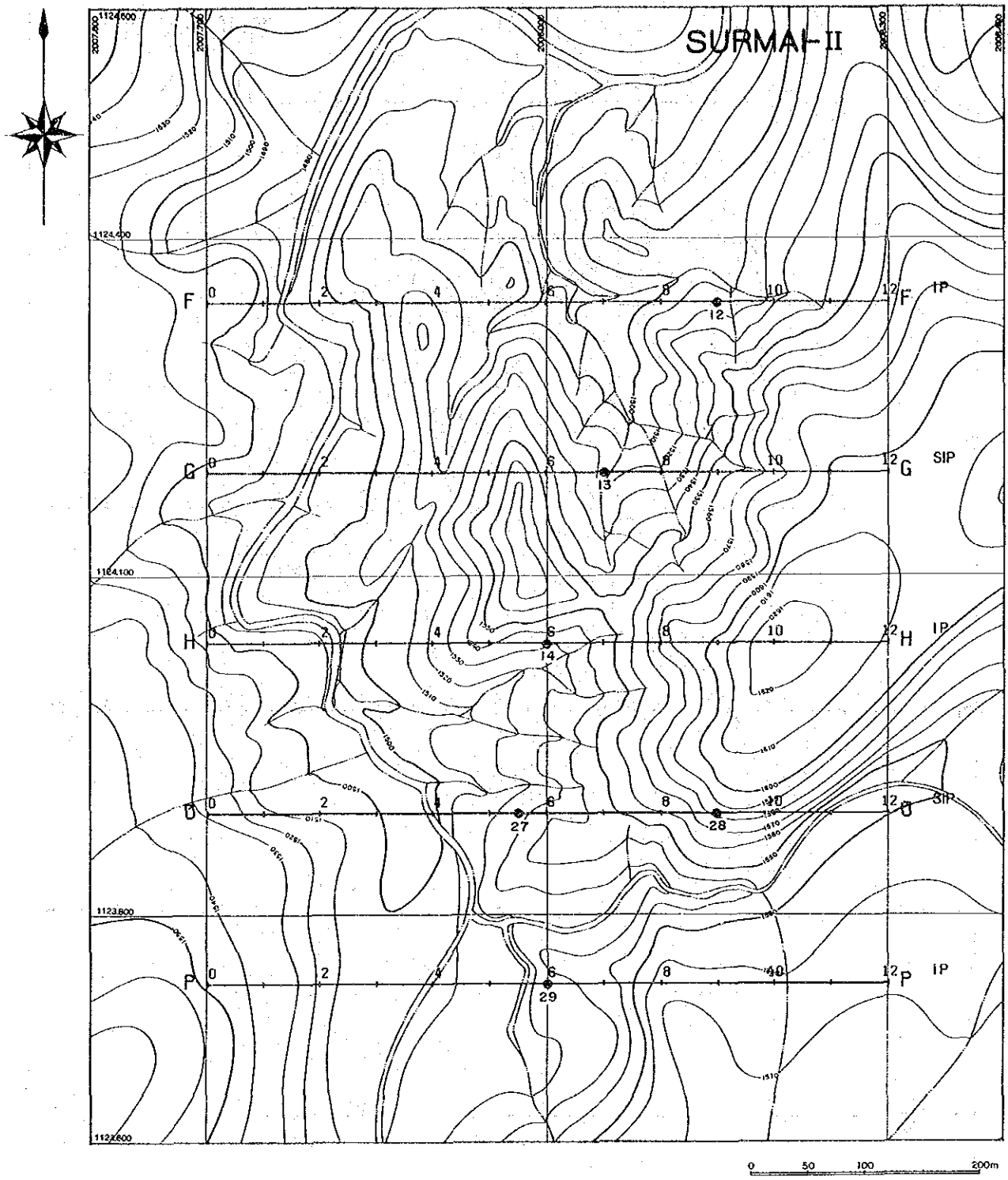

LEGEND

12 Location of Rock Samples

Survey Line

Fig. Ⅲ-3-2 Location Map of Survey Lines in Surmai Ⅱ Area

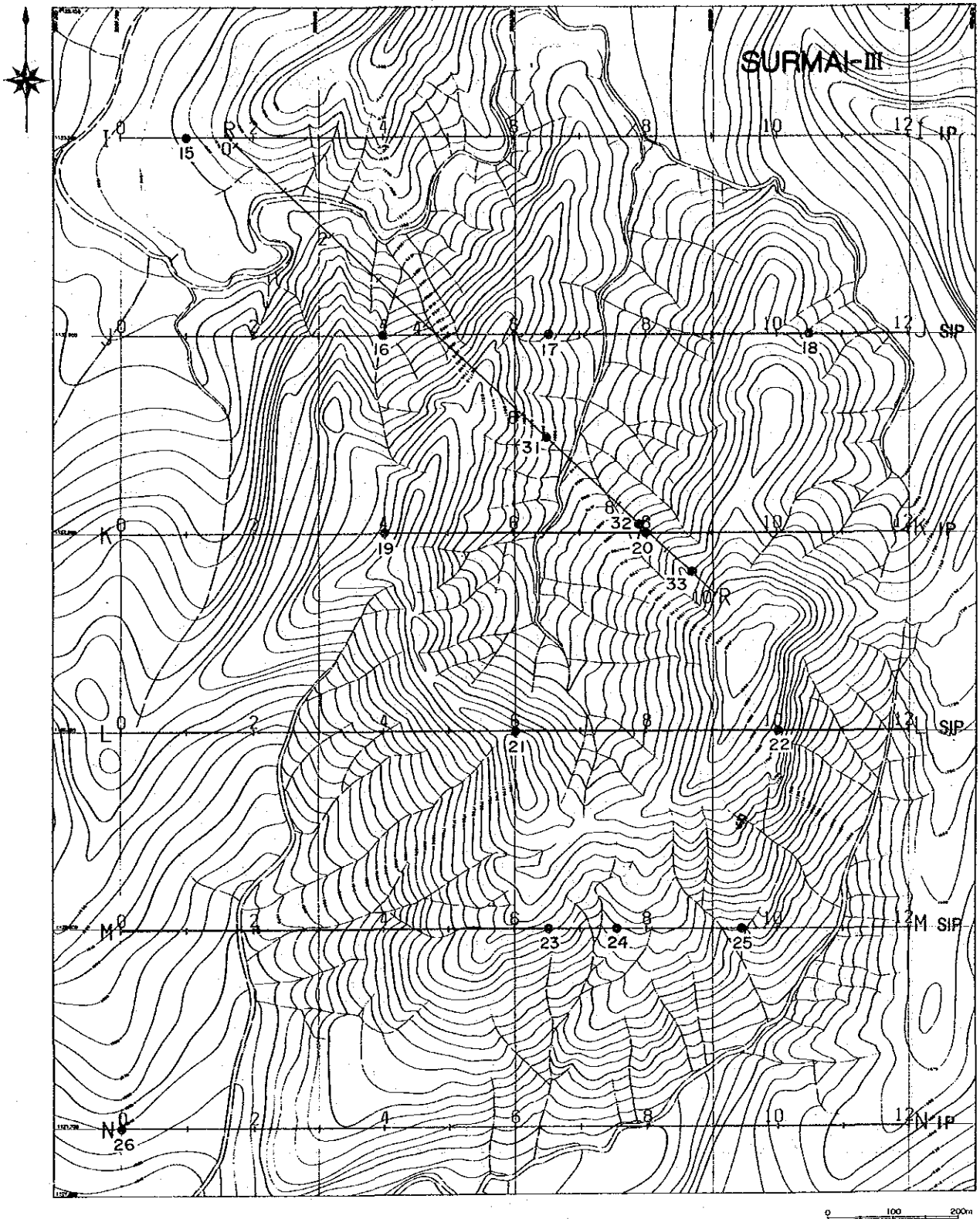

LEGEND

12 Location of Rock Samples

Survey Line

Fig. Ⅲ-3-3 Location Map of Survey Lines in Surmai Ⅲ Area

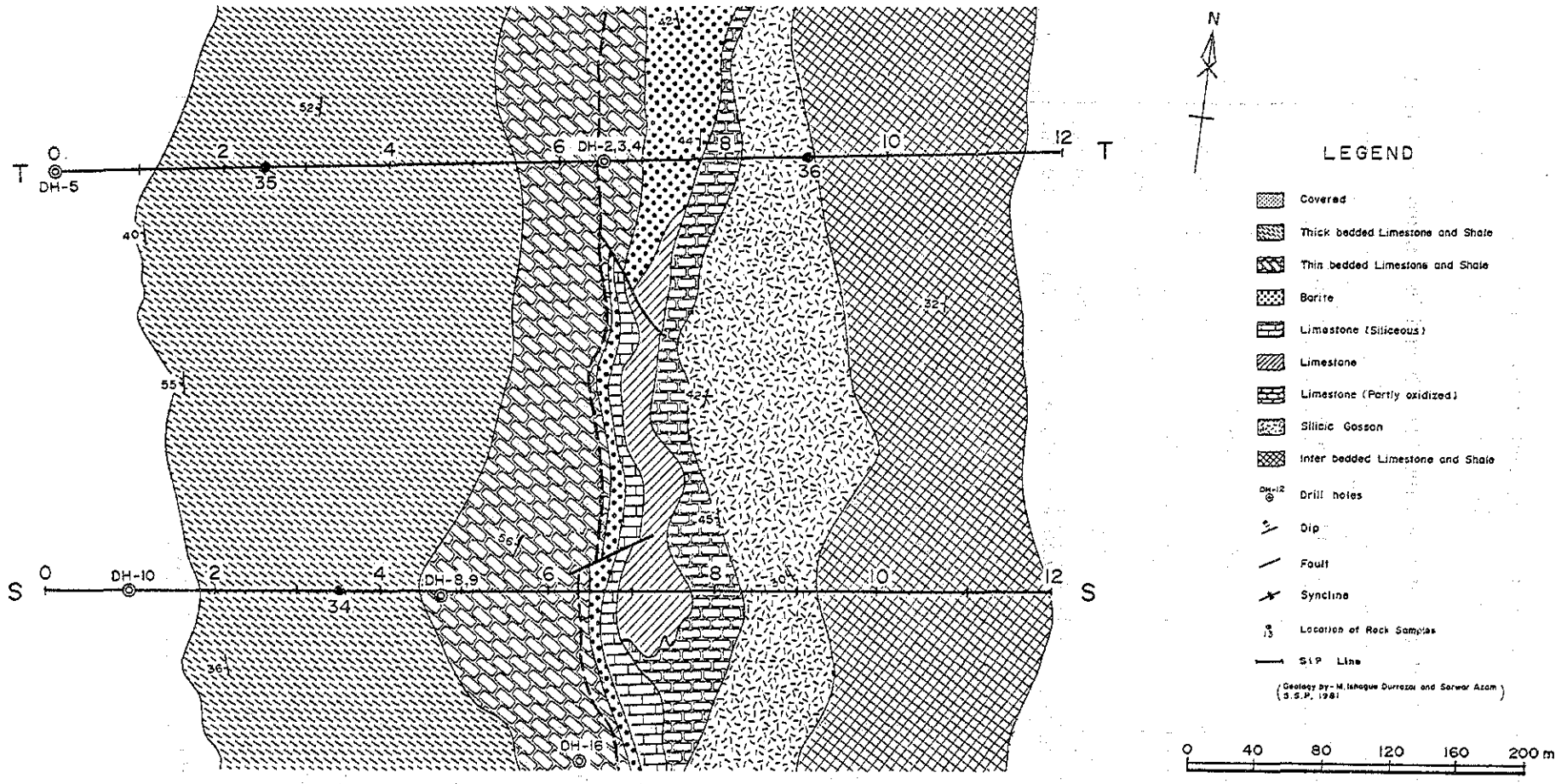

Fig. Ⅲ-3-4 Location Map of Survey Lines in Gunga Mine Area

method measures apparent resistivity and phase difference over a frequency range from 0.01 Hz to 100 Hz, while the conventional IP method measures a

Table Ⅲ-3-1 List of Survey Line Length and Measurement Points

Line	I P		S I P	
	Length	Point	Length	Point
Surmai I Area				
Line A	800 m	60 Ps.		
Line B			800 m	60 Ps.
Line C	800 m	60 Ps.		
Line D			800 m	60 Ps.
Line E	800 m	60 Ps.		
Line Q			800 m	60 Ps.
Subtotal Number	2,400 m	180 Ps.	2,400 m	180 Ps.
Surmai II Area				
Line F	600 m	40 Ps.		
Line G			600 m	40 Ps.
Line H	600 m	40 Ps.		
Line O			600 m	40 Ps.
Line P	600 m	40 Ps.		
Subtotal Number	1,800 m	120 Ps.	1,200 m	80 Ps.
Surmai III Area				
Line I	1,200 m	40 Ps.		
Line J			1,200 m	40 Ps.
Line K	1,200 m	40 Ps.		
Line L			1,200 m	40 Ps.
Line M			1,200 m	40 Ps.
Line N	1,200 m	40 Ps.		
Line R			1,000 m	30 Ps.
Subtotal Number	3,600 m	120 Ps.	4,600 m	150 Ps.
Gunga Mine Area				
Line S			600 m	40 Ps.
Line T			600 m	40 Ps.
Subtotal Number			1,200 m	80 Ps.
Total Number	7,800 m	420 Ps.	9,400 m	490 Ps.

difference in apparent resistivity expressed in percentage of two frequencies. The measurement data are expressed in spectral diagrams of phase and magnitude, and in Cole•Cole diagrams. Analyses of these responses allows discrimination of minerals or types of mineralization and eliminates electromagnetic coupling effects which occur at low resistivity in the ground, at wide electrode separations, and with a large number of electrode coefficients.

In this survey, the Harmonic System of Zonge(USA) was applied. The IP responses over a range of 0.125 Hz to 88 Hz are measured through calculation and extraction of high frequency, using the Fast Fourier Transform of 3rd, 5th, 7th, 9th and 11th harmonics from three basic frequencies of 0.125 Hz, 1.0 Hz and 8.0 Hz.

Observation of a wave form is necessary for measurement of phase , and a communication cable which connects transmitter with receiver was laid down parallel with the survey line separated by 25 m to 30 m. The layout of these lines is shown in Fig.Ⅲ-3-5(a). At the receiving station, response is amplified through three porous pot-electrodes in copper sulphide saturated solution with a copper rod(Fig.Ⅲ-3-5 b). Amplified signals are transmitted through a communication cable to the receiver(GDP-12/2GB). Data is processed and printed out.

The IP method in this survey is that of conventional frequency domain at two frequencies of 0.3 Hz and 3.0 Hz.

3-1-4 Measuring Equipment

The equipment used in this survey are listed in Table Ⅲ-3-2. An illustrated diagram of the equipment is shown in Fig. Ⅲ-3-6.

3－2 Data Processing and Measurement of Rock Samples

3-2-1 I P Data Processing

Panel diagrams of Percent Frequency Effect (PFE) and Apparent Resistivity (AR) were provided from pseudo-sections of each line. Three plan maps were prepared on each electrode separation coefficient of n = 1, 3, 5.

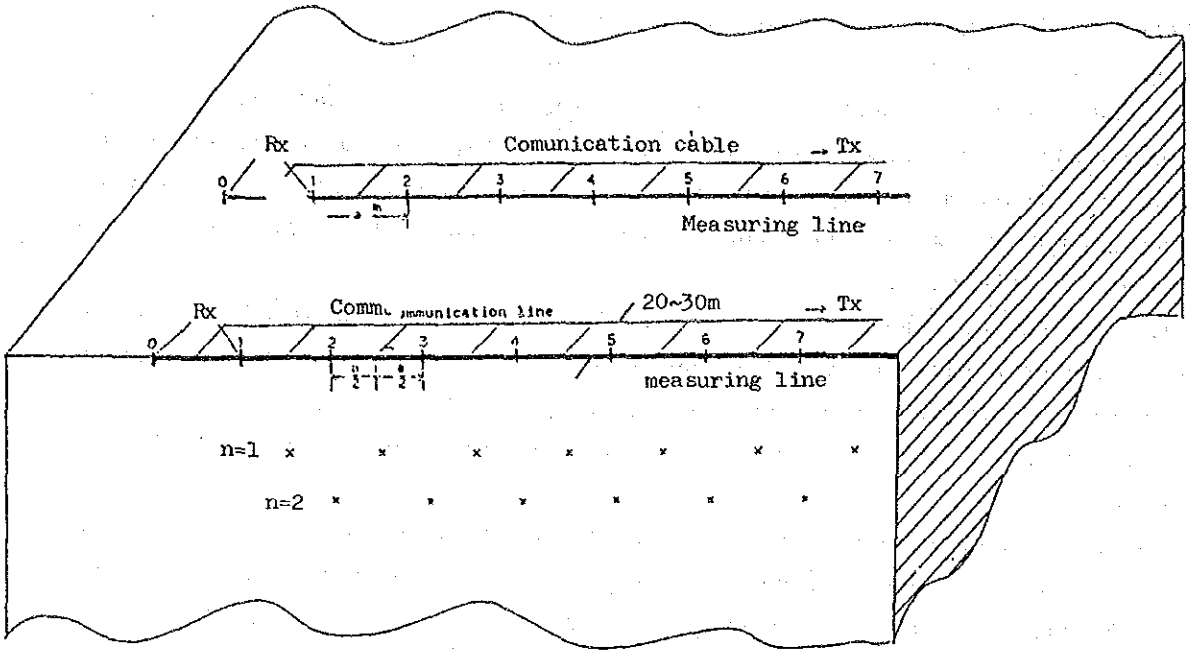

(a) SIP measuring line

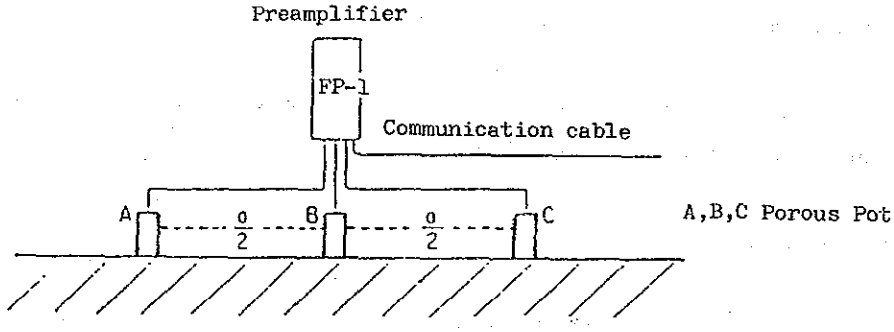

(b) Receiver station

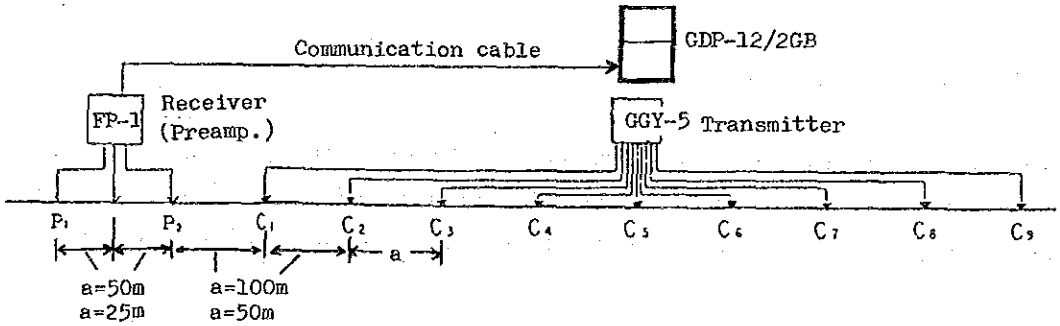

(c) Extention of electrode

Fig. Ⅲ-3-5 Field Work for SIP Measurement

Table Ⅲ-3-2 List of SIP・IP Equipment

ITEM	NAME	SPECIFICATION	QUANTITY
Transmitter System	Chiba Electric CH-86A SIP Transmitter	Output Voltage : 200, 400, 600, 800, 1000V Output Current : 0.2~5.0 A Wave Form : Square wave Frequency : 0.125 Hz~8 Hz Weight : 37 Kg	1
	Zonge XMT-1 Transmitter Controller	Frequency Range : 1/1,024 Hz~2,048 Hz Weight : 5.8 Kg Power : 12V Battery	1
	Chiba Electric Model 8104T IP Transmitter	Output Voltage : 200, 350, 500, 650, 800V Output Current : 0.2~2.5 A Wave Form : Square Wave Frequency : 0.1 Hz~3 Hz Weight : 14 Kg	1
Engine Generator	Zonge ZMG-5 SIP Engine Generator Honda G400	Output Power : 5 KW Frequency : 400 Hz Output Voltage : 115V Engine : 10 hp 4 Cycle	1
	McCulloch MK-II IP Engine Generator	Output : 2 KW Frequency : 400 Hz Output Voltage : 115V Engine : 5 HP 4 Cycle	1
SIP Reciever System	Zonge GDP-12/2GB	Signal Input : 2 Channel Frequency range : 1/8~88Hz (18 Freq.) Senstivity : 0.2μV Weight : 15 Kg Power : 12V Battery	2
	Zonge CAP-12 Mini Cassette/ Tape Racoder	Weight : 6.2 Kg Power : 12V Battery	2
	Tektronx 214 Oscilloscope		1
	Zonge ISO/ Isolation Amp		3
	Zonge FP-1 Field Preamp.		5
IP Reciever	Yokohama Electric YDC-7505B IP Reciever	Frequency Range : 0.1 Hz~3 Hz Sensitivity : 10μV (1, 10, 100, 1000mV) Weight : 3 Kg Power : 006P Battery 4 pcs	1
Electrode	Currrent Potensial	Stainless φ0.6cm, Length 61cm Non Polarizable CuSO4 Porous Pot	200 5

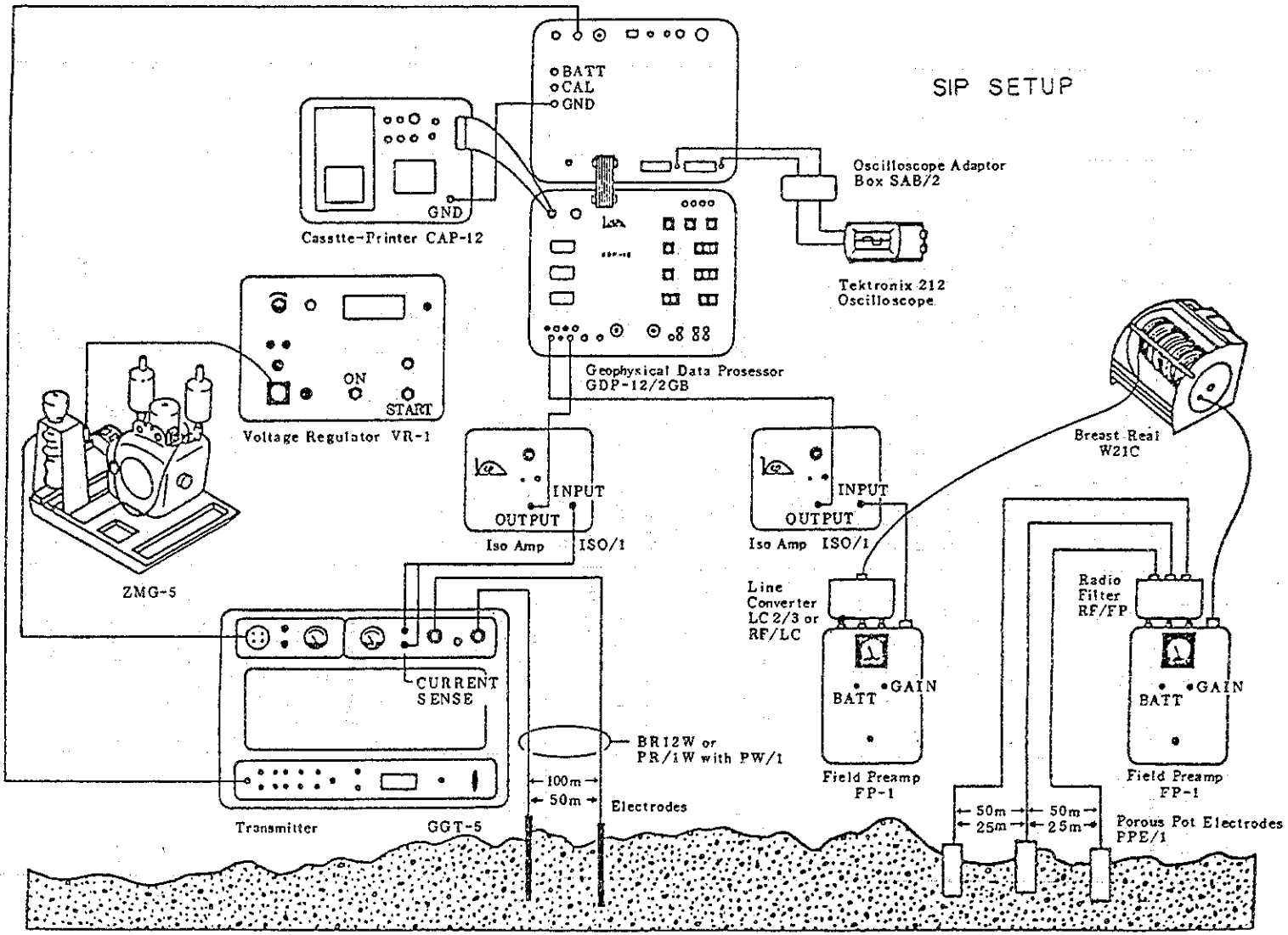

Fig. Ⅲ-3-6 Blockdiagram for SIP Measurement

A) P F E

A value of PFE is calculated using magnitudes (M) of SIP data at 0.125 Hz and 1 Hz and apparent resistivity (ρ a) at 0.3 Hz and 3.0 Hz of IP data as follows :

$$PFE(SIP) = \frac{M(0.125\ Hz) - M(1.0\ Hz)}{M(1.0\ Hz)} \times 100 \quad (\%)$$

or

$$PFE(IP) = \frac{\rho a(0.3\ Hz) - \rho a(3.0\ Hz)}{\rho a(3.0\ Hz)} \times 100 \quad (\%)$$

B) A R

A value of AR is calculated by the following equation :

$$AR = \pi a \cdot n(n+1)(n+2) \cdot V/I \quad (ohm\text{-}m)$$

where, a : electrode separation in meters
n : electrode separation coefficient
V : received voltage in volts
I : transmitted current in amperes

In the present survey, the apparent resistivities of SIP at 0.125 Hz and of IP at 0.3 Hz were calculated and topographic correction was made with conductive paper.

3-2-2 SIP Data Processing

Data obtained in the field consist of real and imaginary parts of complex resistivity responses at each frequency, and apparent resistivity, phase and magnitude of received basic frequency and so on. The following figures were made from these data :

① Cole•Cole Diagram
② Magnitude Spectrum
③ Phase Spectrum
④ Raw Phase at five freqencies
⑤ PFE Pseudo-section
⑥ Apparent Resistivity Pseudo-section

Data processing and method of analysis are given as follows :

A) Cole•Cole Diagram

In a Cole•Cole diagram, print-out data for each frequency are plotted on a coordinate by setting the negative imaginary part on the vertical axis and the positive real part on the horizontal axis. An example is shown in Fig.Ⅲ-3-7. θi and Mi on the figure are, respectively, called phase angle and magnitude. The Cole•Cole diagram is known to display a characteristic spectrum depending on the kind of mineral or rock.

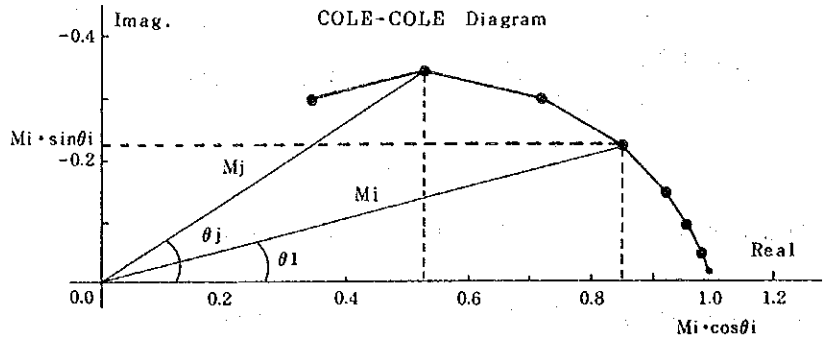

Fig. Ⅲ-3-7 Cole・Cole Diagram

According to Zonge et al, there are three types of spectra as illustrated in the right figure. Type A, showing a pattern of ascent to the right, indicates existence of sulphide minerals, graphite or strong alteration. The flat line pattern of Type B indicates moderate alteration, and the Type C pattern of descent to the right indicates weak alteration, alluvium sediment, fresh igneous rock or limestone.

Discrimination of Cole•Cole diagrams of this survey was based on this classification of the three types.

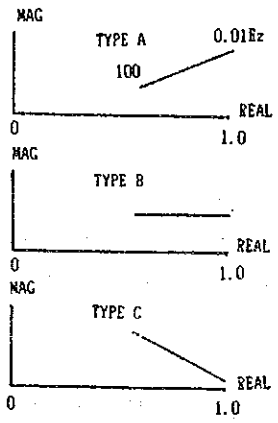

B) Magnitude Spectrum

The magnitude refers to Mi and Mj of Fig.Ⅲ-3-7, and is easily obtained from positive real and negative imaginary components of field data. The values are normalized by dividing by Magnitude M_0 of minimum frequency (0.125 Hz). A magnitude spectrum figure is plotted by setting the magnitude value on the vertical axis and frequency on the horizontal axis (Fig. Ⅲ-3-8). In the figure, a flat line indicates fresh rock without mineralization or alteration, whereas the spectrum line descending to high frequency indicates strong alteration, sulphide minerals and graphite.

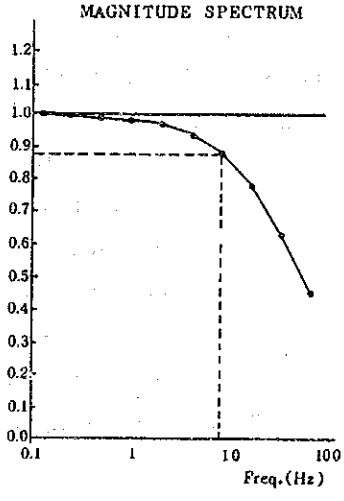

Fig. Ⅲ-3-8 Magnitude Spectrum

C) Phase Spectrum

In the phase spectrum, the vertical axis is phase angle ϕ of Fig.Ⅲ-3-7, and the horizontal axis is frequency. (Fig.Ⅲ-3-9 (a)). Data obtained in the field survey are a combination of original IP responses (solid line A in Fig.Ⅲ-3-9 (b)) and pseudo-IP responses (dotted line B in Fig.Ⅲ-3-9 (b)) derived from electromagnetic coupling. Line C (-x---x-) in Fig.Ⅲ-3-9 (b) shows the combined IP responses. Phase spectrum indicated in Fig.Ⅲ-3-9 (a) was obtained through measurement.

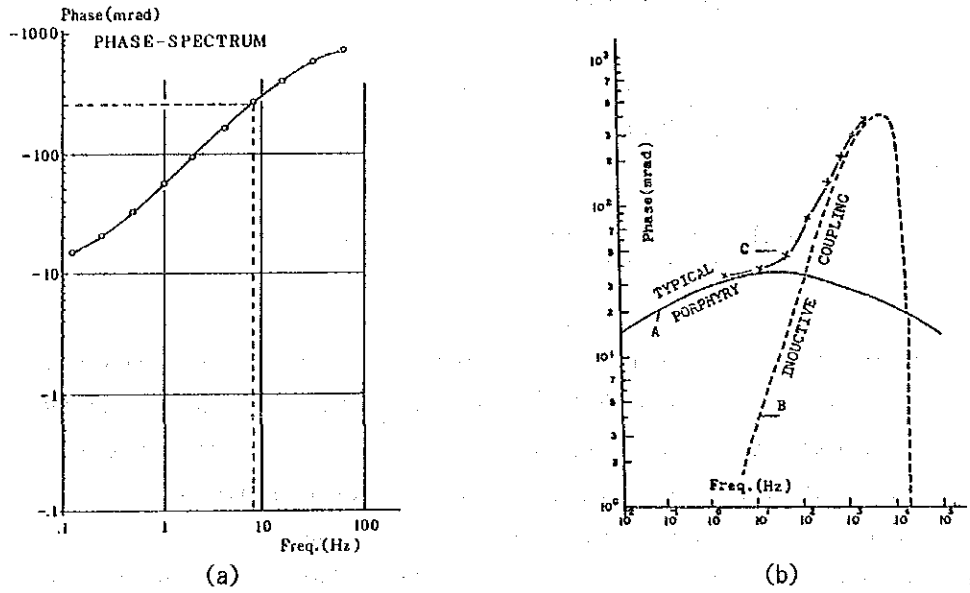

Fig.Ⅲ-3-9 Phase Spectrum

3-2-3 Decoupling Manipulation

Decoupling denotes the removal of a false component in IP responses originating from electromagnetic coupling. The decoupling process was conducted on data over the whole lines of A and B. The decoupling procedure on the SIP measurement in this area was based on the method provided by P.G.Hallof and W.H.Pelton. The analytical method is summarized below. A complex impedance ZA(f) obtained from the SIP survey is approximated by the following equation.

$$ZA(f)=Ro\left[1-m_1\left\{1-\frac{1}{1+(i2\pi f\tau_1)c_1}\right\}-m_2\left\{1-\frac{1}{1+(i2\pi f\tau_2)c_2}\right\}\right.$$

$$\left.+m_3\left\{1-\frac{1}{1+(i2\pi f\tau_3)c_3}\right\}\right]$$

where, m ; chargeability

τ ; time-constant

c ; frequency dependence

f ; frequency

The equation can be separated into three parts as follows ;

$$1-m_1\{1-\frac{1}{1+(i2\pi f\tau_1)c_1}\} \qquad (1)$$

$$-m_2\{1-\frac{1}{1+(i2\pi f\tau_2)c_2}\} \qquad (2)$$

$$+m_3\{1-\frac{1}{1+(i2\pi f\tau_3)c_3}\} \qquad (3)$$

The first nominal refers to an IP response, the second indicates electromagnetic coupling derived from a homogenous earth and the third represents the value of electromagnetic coupling in a conductor. Ten parameters (Ro, m_1, τ_1, c_1, m_2, τ_2, c_2, m_3, τ_3, c_3) of the equation above are determined from the SIP measurement using the least squares method of a non-linear type. The nominals (2) and (3), being the values of electromagnetic coupling, are removed from the equation, and only the complex impedance Zco(f) of the IP response is obtained.

$$Zco(f)=[1-m_1\{1-\frac{1}{1+(i2\pi f\tau_1)c_1}\}]$$

3-2-4 Measurement of Rock Samples

In the analysis and interpretation of the survey results, it is essential to understand the SIP features of main rocks and ores distributed in the surveyed area. The measurement of SIP was conducted over samples totaling 40 pieces to investigate spectra of phase and magnitude, Cole•Cole property, percent frequency effects and resistivities. A location map of samples is shown in Figs. Ⅲ-3-1～Ⅲ-3-4. The procedure of measurement is as follows :

① Sample preparation : A cube of 3 cm is prepared.

② Saturation with water : The samples are soaked in distillied water for 24 hours.

③ Measurement : Instruments used are illustrated in Fig.Ⅲ-3-10. Except for the laboratory transmitter, all instruments and measuring methods are the same as those used in the field. Standard value of current was set at 5～30 μA.

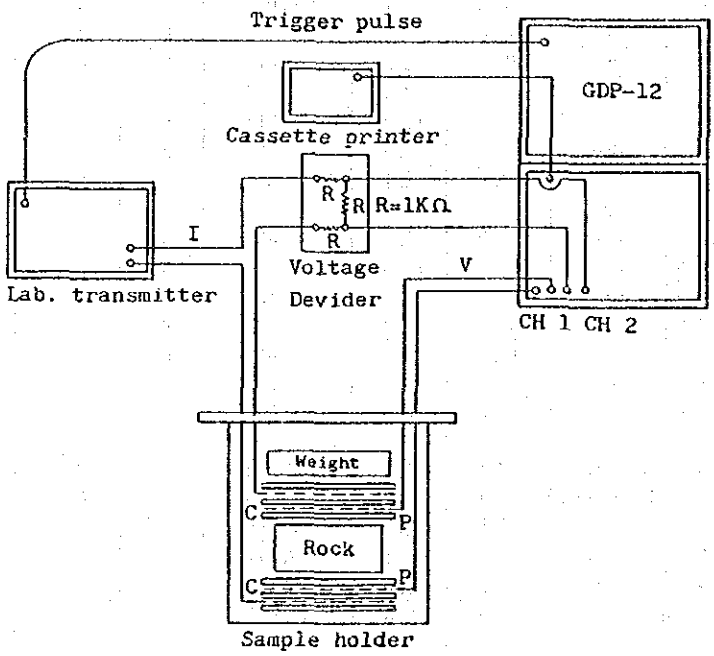

Fig. Ⅲ-3-10 Laboratory Equipment for Rock Sample Measurement

Results of Rock Sample Measurements

Results of the laboratory measurements are shown in TableⅢ-3-3 for total samples, and the spectra of each rock sample are shown in Appendix.

The results from these samples can be categorized by their phase spectra which fall into six types, shown in Fig.Ⅲ-3-11 as A, B, C, D, E, F. The relationship between phase and Cole•Cole spectra is shown in Table Ⅲ-3-4. In comparison, types in the Cole•Cole diagram are divided into two groups: one belonging to type C in the Cole•Cole diagram contains A,B,C and D types of phase spectrum, and the other belonging to type A in the Cole•Cole diagram contains E and F types of phase spectrum.

Table Ⅲ-3-3 Result of Rock Sample Test in Laboratry

Sample No.	Location Line No.	Rock	Phase (-mrad)	P F E (%)	Resistivity (ohm-m)	Spectrum Type Phase	Spectrum Type ColeCole	Remarks
SURNAI AREA								
14	H 6	Ore	39.4	6.0	396	E	A	Anjira II
29	P 6	Ore	26.0	3.7	337	A	B	Anjira II
	Average value		32.7	4.9	367			
13	G 7	Ore	58.1	7.2	390	F	A	Loralai IV
2	B 12	Ore	13.5	2.0	523	A	B	Loralai III
4	C 10	Ore	30.2	3.7	4,090	D	C	Loralai III
5	C 11	Ore	31.6	4.2	1,173	B	B	Loralai III
8	D 9	Ore	40.0	5.5	675	B	B	Loralai III
26	N 0	Ore	12.5	2.5	329	E	B	Loralai III
3	B 15.5	Ore	93.8	11.2	816	F	A	Loralai II
16	J 4	Ore	14.8	2.3	695	A	C	Loralai II
19	K 4	Ore	24.0	3.1	676	A	B	Loralai II
20	K 8	Ore	18.6	2.7	403	A	B	Loralai II
22	L 10	Ore	13.9	1.9	2,465	A	C	Loralai II
23	M 6.5	Ore	103	14.8	291	E	A	Loralai II
25	M 9.5	Ore	99.3	13.1	198	E	A	Loralai II
32	R 8.5	Ore	37.7	5.0	1,822	B	B	Loralai II
33	R 9.5	Ore	11.3	1.7	612	E	C	Loralai II
11	E 11	Ore	27.2	3.3	575	B	B	Loralai I
	Average Value		39.3	5.3	983			
27	O 5.5	Limestone	9.1	1.2	2,253	B	B	Anjira II
6	D 1	Limestone	0.7	0.1	16,646	A	B	Anjira II
15	I 1	Limestone	3.5	0.5	6,266	A	B	Anjira II
7	D 5	Limestone	11.2	1.7	2,777	A	B	Anjira I
12	F 9	Limestone	3.2	0.5	25,405	A	C	Anjira I
	Average Value		5.5	0.8	10,669			
1	A 8	Limestone	3.2	0.5	15,336	A	B	Loralai IV
10	E 1	Limestone	4.8	0.7	15,670	C	C	Loralai IV
28	O 9	Limestone	5.4	0.8	8,051	C	C	Loralai IV
30	Q 8.5	Limestone	2.6	0.4	11,371	A	B	Loralai IV
18	J 10.5	Limestone	5.2	0.9	5,785	A	B	Loralai III
24	M 7.5	Limestone	7.0	1.0	14,200	A	B	Loralai III
9	D 11	Limestone	6.3	0.9	8,920	A	C	Loralai II
17	J 6.5	Limestone	7.6	1.0	12,734	D	C	Loralai II
21	L 6	Limestone	5.2	0.7	4,244	A	B	Loralai II
31	R 6.5	Limestone	3.1	0.4	23,648	D	C	Loralai II
	Average Value		5.0	0.7	11,99			
GUNGA MINE								
37	Gunga M.	Ore	15.8	2.3	293	E	B	Anjira II
36	T 9	Ore	42.0	5.7	704	A	B	Anjira II
	Average Value		28.9	4.0	499			
38	Gunga M.	Barite	0.5	0.1	22,636	D	-	Anjira II
39	Gunga M.	Barite	1.9	0.3	3,024	E	B	Anjira II
40	Bunga M.	Barite	0.5	0.02	15,666	E	-	Anjira II
	Average Value		1.0	0.1	13,776			
34	S 3.5	Limestone	13.1	2.0	6,221	B	B	Anjira III
35	T 2.5	Limestone	9.5	1.3	10,232	B	B	Anjira III
	Average Value		11.3	1.7	8,227			

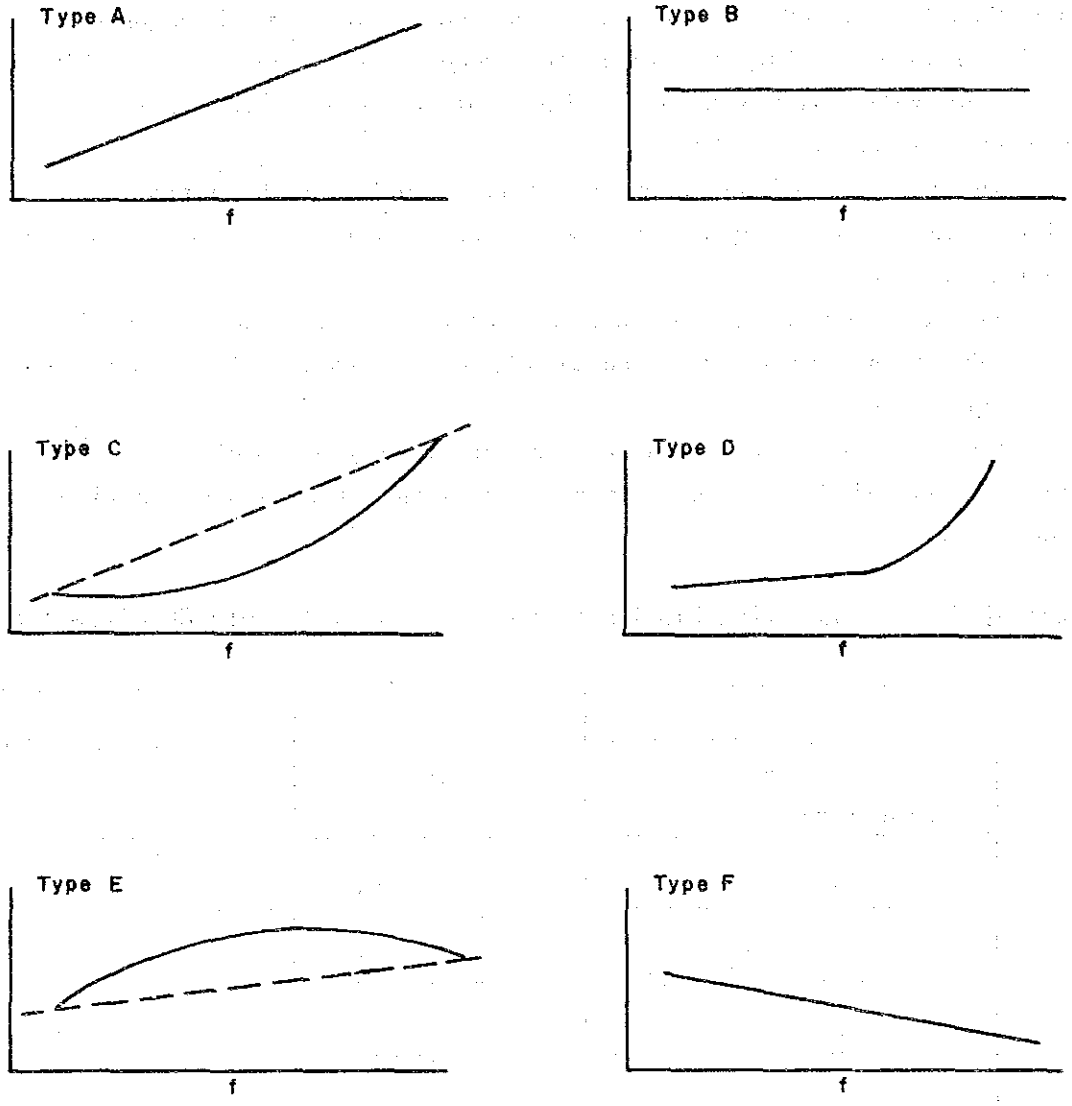

Fig. Ⅲ-3-11 Phase Spectrum Types of Rock Samples

The result indicates the following :

① Phase and PFE of ores are 7 times higer than those of limestones.
② Phase and PFE are proportionately correlated. Samples indicating more than 5% in PFE have big values of more than 30 mrad in phase.
③ Resistivity values are in a wide range from 198 ohm-m to 25,405 ohm-m. Most values are generally high, but 8 samples (20 % of all the samples) are below 500 ohm-m.
④ In the case of the phase spectrum, samples of high phase and PFE belong to E and F types, and resistivity is not correlated with the phase spectrum.
⑤ On the other hand, the rock samples of limestone are higher than 2,000 ohm-m in resistivity, and mostly belong to A and D types of the phase spectrum.
⑥ The samples of barite show high resistivity and low PFE values,and there is no difference of geophysical properties between barite and limestone.

Table Ⅲ-3-4 Relationship between Phase and Cole・Cole Spectrum Type

Cole•Cole Type / Phase Type	A	B	C	Total No.
A	-	13	4	17
B	-	7	-	7
C	-	-	2	2
D	-	-	3	3
E	3	2	1	6
F	2	-	-	2
Total Number	5	22	10	37 (1)

(1) Three samples of Barite are excepted,because that Cole•Cole spectrum is not clear.

3-3 Results of Interpretation

Survey results over the Surmai area are put together as follows.

Each plan and section of apparent resistivity (AR) and percent frequency effect (PFE) are compiled with data on survey lines for SIP and IP measurements. The plans on AR and PFE at an electrode separation index of n = 1, 3, or 5 are provided for each area of Surmai I to III. Panel diagrams of each area are prepared, comprising of sections of AR and PFE on each survey line.

In regard to SIP responses, pseudo-sections of phase lag, phase spectrum and magnitude spectrum, and Cole•Cole diagrams at five frequencies ranging from 0.125 to 3.0 Hz for each line are drawn.

Discussions on the survey results are given, based on those drawings.

3-3-1 Plan Map and Pseudo-Section of Apparent Resistivity(AR)

The AR in the Surmai area ranges from 1.9 to 2,247 ohm-m, averaging at 83 ohm-m. The standard deviation (σ) after common logarithms stands at 0.494, giving M+σ and M-σ of 260 ohm-m and 26.7 ohm-m. Consequently, contour values of 300 and 30 ohm-m are deemed as criteria, being approximations of the above, to distinguish high and low resistivities.

Surmai I

AR plan : Fig.III-3-12 (1) to (3)

A zone of low AR extends in a N-S direction in the middle of the area, corresponding roughly with the distribution of Unit IV of the Anjira Member.

Noticeable zones of high AR are observed in the northeastern part of the area on the plan at n=1 and in the northwestern part on the plans at n=3 and 5.

AR section : Fig.III-3-13

A zone of low AR of less than 30 ohm-m exists in the middle of each line, except Line Q. The western margin of the zone approximately coincides with the boundary between the Anjira and Loralai Members. Zones of high AR have been detected at the western ends of Lines A to E and at the eastern ends of Lines B to E. A zone of low AR lies between the zones of high AR at the eastern end of Line C, giving a sandwich structure.

Surmai II

AR plan : Fig.III-3-14 (1) to (3)

A prominent zone of low AR has been observed at the eastern end of the plan at n=1, along the boundary between Units II and III of the Loralai Member. Small zones are noticed at the southeastern part on the plan at n=3 and at the northern part of the middle on the plan at n=5.

AR section : Fig.III-3-15

Zones of low AR have been detected on all sections from Lines F to P, in a small area on the eastern side of each line. To the south of Line G, the area becomes larger as it proceeds southward. The zones are observed along Unit IV of the Loralai Member.

Surmai III

AR plan : Fig.III-3-16 (1) to (3)

On the plan at n=1, zones of high AR are prominent in the northwest and southeast. At n=3, a zone of low AR in the east and a zone of high AR in the middle are obvious. At n=5, a small zone of low AR has been detected in the north. Those zones of both high and low AR are distributed in a N-S direction.

AR section : Fig.III-3-17 (1) and (2)

Zones of low AR dominate the area between Lines K and L. High AR locally shows small distribution. In contrast, zones of high AR exist in the middle of each line from Lines L to M. The area is underlain by the Loralai Member except in the northwest where the Anjira Member occurs. Discrimination of these two Members by a distribution of AR seems to be difficult due to a small difference in resistivities.

3-3-2 Plan Map of Pseudo-Section of Percent Frequency Effect(PFE)

The value of PFE in the Surmai area ranges from -8.3% to 5.2% with an average (M) of 0.66% and a standard deviation (σ) at 0.772, giving M+σ and M+2σ of 1.43% and 2.20% respectively. A histogram with an interval of 0.5% shows a normal distribution for the most part. In the laboratory measurements, limestone gives PFE of less than 0.7%. Accordingly, a value around M+σ, at more than 1.5%, is referred to as weakly anomalous, and one around M+2σ, at more than 2.5%, as anomalous.

Based on these criteria, zones of weakly anomalous and anomalous are extracted from PFE plans and sections.

Surmai I

PFE plan : Fig.III-3-18 (1) to (3)

Anomalies of this area are detected in the northeast and northwest.

The anomaly in the northeast accords with gossans which are distributed in a NE-SW direction over an area of Lines B, C and D. It is detected on Lines B and C of the plan at n=1, and on Lines B and C and in the middle of Lines C, D and E of the plan at n=5. A negative PFE is accompanied with this anomaly, being the negative maximum of -8.3% on Line B of the plan at n=3. The anomaly in the northwest is found mainly on Lines A to C, extending in a N-S direction. The largest value in the area is recorded as 5.2% PFE on No.2 in Line C on the plan at n=1. On the plan at n=5, a weakly anomalous area reaches to Line D, continuing in a NE-SW direction.

The area of this anomaly coincides with the area of Unit II of the Anjira Member.

PFE section : Fig.III-3-19

To be noticed are detected anomalies in the lower portion of Nos.10-13 on Line B, No.2 on Line C, Nos.9-11 and Nos.13-14 on Line C, and Nos.6-9 on Line D. Especially, anomalies on the lower extension of the mineralized zone delineated at the surface, are continuous to No.10 on Line B, No.10 on Line C and Nos.6-9 on Line D. Negative values of PFE are detected, being correlative with low AR of less than 10 ohm-m, at the lower portion of No.12 on Line B and Nos.13-14 on Line C.

Surmai II

PFE plan : Fig.III-3-20 (1) to (3)

A weakly anomalous zone extends in a N-S direction at the central part of the area. The contour line of 1% runs for the most part along the boundary between the Anjira and Loralai Members. The zone accords with the distribution of the mineralized zone in the area. Two weak anomalies are observed in the middle of Lines F and G on the plan at n=3 and one anomaly is detected in the central part of Lines H and O. On the plan at n=5, weak anomalies are seen sporadically on Lines F,G and O and do not form a definite anomalous zone.

PFE section : Fig.III-3-21

Weak anomalies of more than 1.5% are detected, dipping to the west. Among them, the anomaly on Line F extends from shallow depth to the deep and is large in scale. All anomalies of this area are located in the boundary between the Anjira and Loralai Members, and coincide with small mineralized zones along a N-S trending fault.

Surmai III

PFE plan : Fig.III-3-22 (1) to (3)

Anomalous areas are delineated in the northwestern and the southwestern part of the middle. On the plan at n=1, weak anomalies are detected in the western ends of Lines I and J where the ore horizon of the Gunga Mine, the Anjira Member, occurs. Negative values of PFE are obtained in the east of Lines K and M. On the plan of n=3, weak anomalies are found at the intersection of Lines J and R and in the vicinity of No.8 on Line L, being situated in the lower extension of the mineralized and altered zone. The weak anomalies of the Anjira Member is not seen. The plan of n = 5 gives a high PFE of 3.2% at No.4 on Line J, and 2.3% in the vicinity of No.8 on Line J. These are deemed to be the lower extensions of anomalies detected on the plan of n = 3.

PFE section : Fig.III-3-23 (1) and (2)

A distribution of PFE of each line is shown in a panel diagram to delineate form and depth of origin of anomaly. To be noted are anomalies of the lower portions of No.4 on Line J and Nos.7-8 of Line L. The former enlarges towards depth and the latter is a vertical anomaly. Areas of negative PFE are broadly detected on Lines I,K,M and N, which are not seen in Surmai I or II.

3-3-3 Pseudo-Section of Phase

Sections are provided for each phase of 0.125, 0.375, 0.625, 1 and 3 Hz to investigate reliance of phase on frequency (Fig.III-3-24 to III-3-32). Phase sections after decoupling are also shown.

The phase section of 0.125 Hz before data processing is correlative with the PFE sections, as being pointed out that an area of high PFE gives a larger phase. The value of phase becomes slightly larger in accordance with an increase of frequency from 0.125 Hz with an effect of electromagnetic coupling which is negligible in the area. The effect of electro-

magnetic coupling in this field is very small due to the existence of highly resistive limestone of Jurassic age.

The phases of each frequency after decoupling are almost the same as the ones at 0.125 Hz before data processing, and an effect of electro-magnetic coupling which could be faintly noticed is eliminated by decoupling procedure.

3-3-4 Phase, Magnitude and Cole•Cole Spectrum

Pseudosections of phase spectra, magnitude spectra and Cole•Cole diagrams are prepared on each of survey lines for the SIP method. Diagrams of various spectra after decoupling are also shown.

Phase spectra:

In general, phase spectra of A- and D-types predominate (Fig.Ⅲ-3-11). These types are common in rocks of high resistivity with low PFE, such as limestone and shale. In the areas where PFE anomalies are detected, values of phase exceed 10 mrad. In the field of high frequency of more than 10 Hz, spectra of high inclination are observed due to slight electro-magnetic coupling.

In the areas where negative PFE are detected, plus-minus signs of phase are also converse and spectra are unique, being of V-type. These phenomena occur at (1) Nos.10-14, Line B, (2) Nos.7-10, Line D, (3) Nos.3-5, Line J, and (4) Nos.3-5 & 9-10, Line M.

Phase spectra after decoupling are almost of flat-lying B-type due to the elimination of electro-magnetic coupling in the field of high frequencies. A part of negative phase has also disappeared. Areas of high PFE give spectra which are flat-lying or slightly slanting up to the right hand side with higher initial values of phase, showing obvious anomalous areas. Spectra of E- and F-types which are noticed on gossans in the laboratory measurements of rock properties, are found at depth at No.5 on Line B.

Magnitude spectra:

Flat-lying spectra are dominant, running closely with the axis of abscissas. In depths of more than n = 3, spectra have a tendency to slant down.

Magnitude spectra after decoupling are almost horizontal in the shallow part and also at depth. Downward slanting spectra have been preserved in areas of high PFE or of large phase, probably due to an IP characteristic

other than electromagnetic coupling.

Cole•Cole diagram:

The downward slanting type of C dominate(see 3-2-2). Most spectra are composed mainly of a real part with a small imaginary part. Consequently, line lengths of spectra are short, especially after decoupling, where spectra are represented by dots, because imaginary parts become nil.

A sharp-rising, long spectrum is obtained before decoupling, in the lower part of Nos.10-11 on Line B. This is not an anomalous spectrum related to mineralization, but is assumed to have originated from electromagnetic coupling caused by wiring during the field measurement.

3-3-5 Decoupled SIP Data

Phase, magnitude and Cole•Cole diagrams after decoupling have already been presented and discussed with data before processing.

Because of high resistivities in the area, it can be supposed that an effect of electro-magnetic coupling originating from the ground would be fairly small, and this is confirmed by the fact that large differences are not recognized in the values of phase at five frequencies ranging from 0.125 to 3 Hz between data before and after processing. Slight electromagnetic coupling of more than 10 Hz is known in the field but this is almost completely eliminated by decoupling. In the field of more than 10 Hz after data processing, phase spectra and magnetude spectra are almost identical with those of the field of low frequency of less than 10 Hz.

3-3-6 Model Simulation for IP Anomaly

Anomalies discussed above are ones qualitatively found or evaluated on the pseudo-sections. As a quantitative analysis, locations of anomaly sources and values of PFE and AR are investigated by simulation of models.

The simulation is conducted on main anomalies delineated on Lines C and D of Surmai I and Lines J and L of Surmai III areas.

Line C : Fig.III-3-42

Gossans occur between Nos.11 to 13 on this line and weak anomalies have been found below the outcrops. Similar anomalies are seen at depth at No.2, Nos.4 to 6 and Nos.13 to 14.

The gossans are coded as 2 (10 ohm-m, 5%), and Code 5 (100 ohm-m,10%)

is allocated to an assumed primary orebody. The anomaly at shallow depth at No.2 and the anomaly between Nos.5 and 6 related with Unit II of the Anjira Member are coded as 2 and 3 (200 ohm-m, 3%) respectively.

The results of simulation accord reasonably with the field measurements and indicate an existence of the primary ore deposits about 80 m wide at a depth of some 150 m from the surface.

Line D : Fig.III-3-43

The southwestern extension of gossans on Lines B and C is known between Nos.9 and 10, and its anomaly is detected in the western side at depth between Nos. 6 and 8. Code 3 (50 ohm-m, 10%) is set for a lower part between Nos.4 and 6, and Code 2 (100 ohm-m, 1.5%) is given to the gossans of the simulation model. Results fit in well with the field measurements and the model is deemed to be adequate. An expected orebody may be located between Nos.4 and 6 at a depth of 80 to 100 m from the surface.

Line J : Fig.III-3-44

The most promising anomaly in the Surmai III area is obtained on this line. The gossans between Nos.4 and 5 and the anomaly at depth at No.8 are coded as 2 (10 ohm-m, 8%) and Unit 1 of the Anjira Member is given Code 6 (10 ohm-m, 0.5%). The results of the simulation are harmonious with patterns of field data. The primary body below the gossans is estimated to be about 150 m wide at a depth of 250 m from the surface.

Line L : Fig.III-3-45

The anomaly is located in the eastern extension of gossan between Nos.5 and 7. The primary zone is represented by Code 3 (50 ohm-m, 7%) and a similar anomaly source with the same properties is set beneath the section between Nos.10 and 12. The results of the simulation give a pattern which was harmonious with the field measurments. Ore depths are assumed to be some 100 m.

Resulting locations, depths and widths of primary ore zones are shown in Table III-3-5.

3-3-7 Discussion and Interpretation Map

Mineral showings in the Surmai area are found in three places with various dimensions of mineralized zones. They are comparatively small in scale in the areas of Surmai I and II, and measurements were carried out

Table Ⅲ-3-5 Result of Model Simulation for SIP・IP Anomalies

Line	Location	Depth	Width
C	Nos.9-11	135 m	80 m
D	Nos.4-6	75-100 m	60 m
J	Nos.3-5	200 m	200 m
	Nos.8.5-10	170 m	165 m
L	Nos.5-6	100 m	30 m
	Nos.9-12	100 m	65 m

with station intervals of 50 m and line spacings of 150 m. Station intervals of 100 m with line spacings of 300 m were adopted in the area of Surmai Ⅲ, because the mineralized zone there was large in scale and seemed continuous in its extension. Therefore, information on the depths stands at up to some 150 m deep in the areas of Surmai Ⅰ and Ⅱ, and up to about 300 m in the Surmai Ⅲ area. Lines were spaced as broadly possible, because main geological structures in the areas are continuous in a N-S direction. The following interpretations are drawn from the results of the field survey, measurements of rock properties and analyses of spectra.

(1) The apparent resistivity in the Surmai area ranges from 1.87 to 2,247 ohm-m with an average of 83 ohm-m. According to the measurements of rock properties, gossanous ore of the Anjira Member has a 367 ohm-m resistivity and one of the Loralai has 11,996 ohm-m in average. Limestone of the Anjira gives 10,669 ohm-m and one of the Loralai gives 11,996 ohm-m in resistivity, four to ten times larger than values obtained in the field. This may be due to a low resistivity of sediments such as sandstone and shale ranging from several to several tens of ohm-m in a wet condition, although the properties have not been measured because of difficulties in preparation of specimens of weathered rocks, and also due to a low resistivity of limestone beds in which all cavities are filled with water. At the beginning of the

survey, difficulties with measurements were expected for arid conditions which often prevent a current of electricity. Actually, the current of 0.5 to 2.5 amperes passed through probably on account of moisture content above the previous expectation. The existence of ground-water contributed largely to the field measurements.

(2) Gossanous ores of the Anjira and Loralai Members are 5% in PFE, and limestones of these members stand at 0.8 and 0.7% respectively. Consequently, the non-oxidized primary zones expected beneath the gossans may show larger IP effects. In general, the Mississippi Valley-type ore deposits are said to be formed by hydrothermal replacement comprising mainly of lead and zinc minerals with a few pyrites, and because of an existence of IP effects derived from galena, IP and SIP methods are effective in exploration of this type of deposit.

Especially as observed in this type of ore deposit, where mineralization occurs in sediments such as limestone and shale, and is restricted to areas such as cavities, crushed zones or fractures in limestone, it becomes possible to delineate the mineralization due to contrasts of IP and SIP effects between ores and wall rocks even if the effects are not so large. Detected IP anomalies in this area are almost all located in lower extensions of gossans and are assumed to be of IP anomalies originating from mineralization in the primary zone.

(3) Weak anomalies are obtained on the boundary between Members of the Anjira and Loralai, and in Unit I of the Anjira Member. As no sulphide minerals or graphite have been found under the microscope or by the X-ray analysis, they are assumed to be related with faults or fractures. An anomaly of 5.2% PFE at the lower part of No.2 on Line C in the Surmai I area is also considered to have originated from a fault running in a N-S direction at the eastern side.

(4) On the eastern ends of Lines B and C in the Surmai I area, PFE anomalies are accompanied with negative FE anomalies. They can be related to mineralization along bedding cleavages and small faults in Unit I of the Loralai Member, but their scale and grade seem to be small and low.

(5) In the Surmai III area, negative FE are broadly delineated on Lines I, K, M, and N. They are often located at the contact between high and low resistive bodies, but this does not account for the FE in this area

as the traverse lines have been laid down perpendicular to the trend of geological structures and no faults or fractures have been located parallel with the lines. The instruments used for IP and SIP surveys were common in three areas but only IP lines of I, K and N in Surmai III gave a series of negative FE. Therefore, the phenomenon does not depend on a specific instrument.

The results of field survey and analyses are compiled in diagrams of the analytical interpretation. Typical distributions of apparent resistivity and per-cent frequency are given and locations of origins of IP obtained by simulation are illustrated in the diagrams. The results of the investigation are summarized as follows.

Surmai I :

(1) Prominent IP anomalies are delineated on Lines B, C and D in the depths of gossans in the east. Origins are located by simulation to a depth of some 130 m on Line C and about 75 m on Line D, with the resistivity ranging from 50 to 100 ohm-m and 10% FE.

(2) Anomalies with negative FE on the eastern ends of Lines B and C are related with mineralization along the bedding planes and small faults in Unit I of the Loralai Member in the southeast, but the scale and grade of orebody are not promising.

(3) The high PFE at the western end of Line C seems to be related to an anomaly in the fault. Not being continuous to adjacent lines, mineralization seems to be local.

(4) No anomaly of PFE is detected on Line Q laid down in the middle between Surmai I and II, and only a small increase in PFE is noticed below Nos.6 to 7. No continuation of mineralization can be expected between these areas.

Surmai II :

(1) A N-S trending weak anomaly is delineated in the centre of the area. The anomaly is conspicuous on Lines F and G in the north, but surface expression does not give much anticipation of scale and grade.

Surmai Ⅲ :

(1) Remarkable PFE anomalies are delineated on Lines J and R in the northwest and L in the middle.

(2) The former is situated in the extension of the most prominent gossans and is affirmed on Line R which runs at a right angle to the trend of the mineralized zone. Simulation gives an origin of 10 ohm-m with 8% PFE at a depth of about 200 m from the surface.

(3) The latter is located along a fault in the east of the lower extension of gossans between Nos.6 and 7. Simulation indicates an existence of the anomaly origin of 50 ohm-m with 7% PFE at the bottom between Nos.9 and 12.

(4) Negative FE is broadly detected on IP traverse lines of this area.

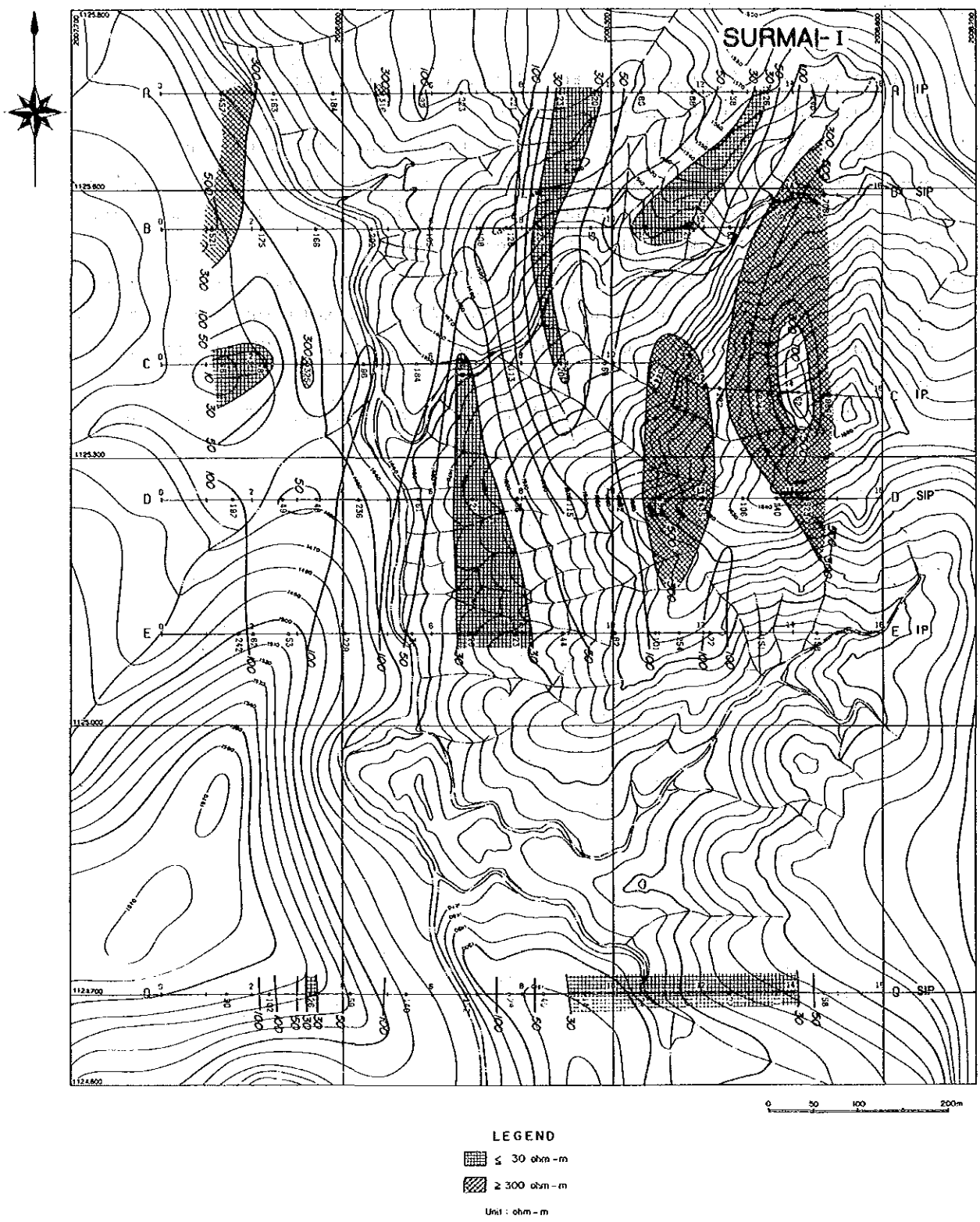

Fig. Ⅲ-3-12(1) Plan Map (n=1) of Apparent Resistivity in Surmai I Area

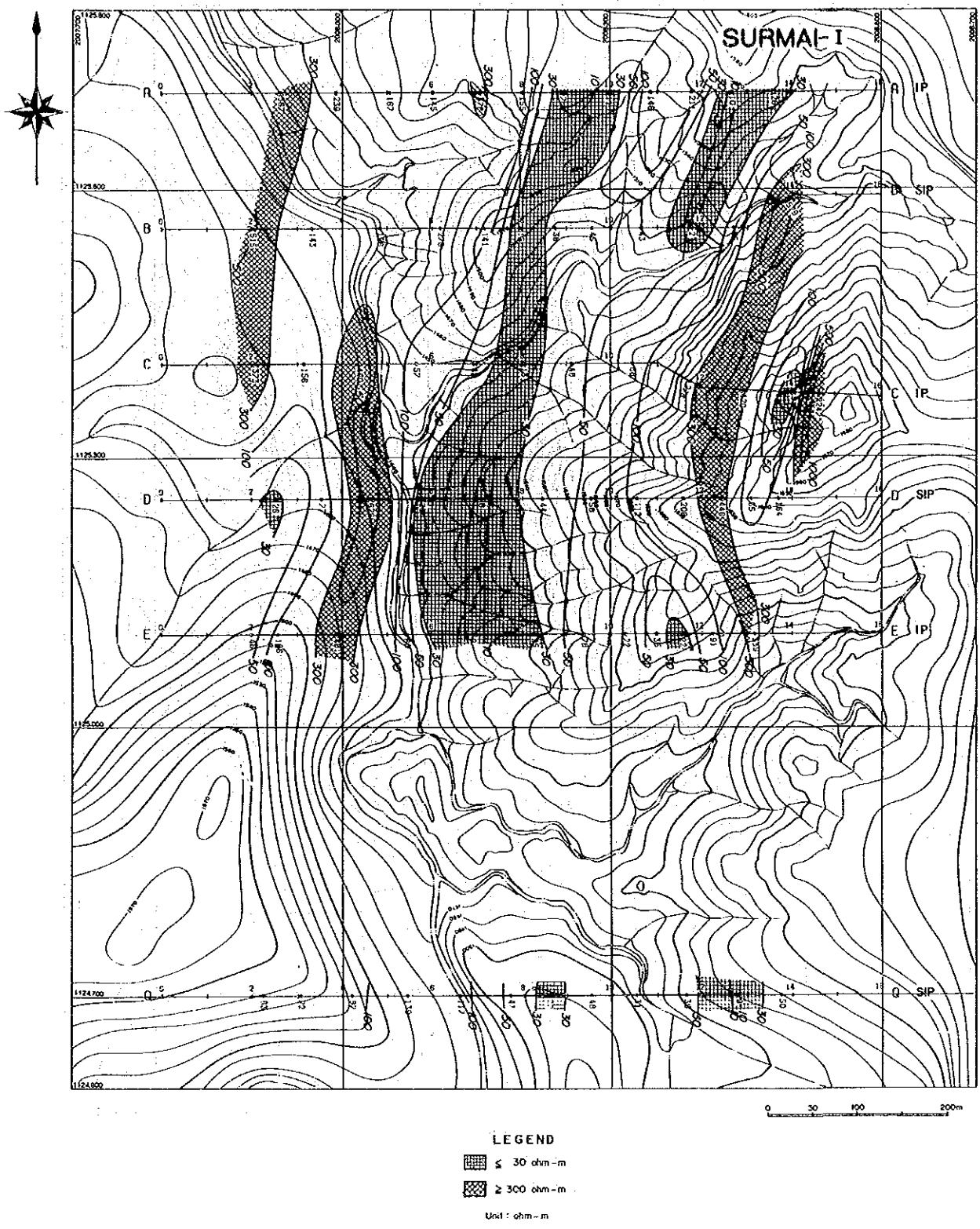

Fig. Ⅲ-3-12(2) Plan Map (n=3) of Apparent Resistivity in Surmai I Area

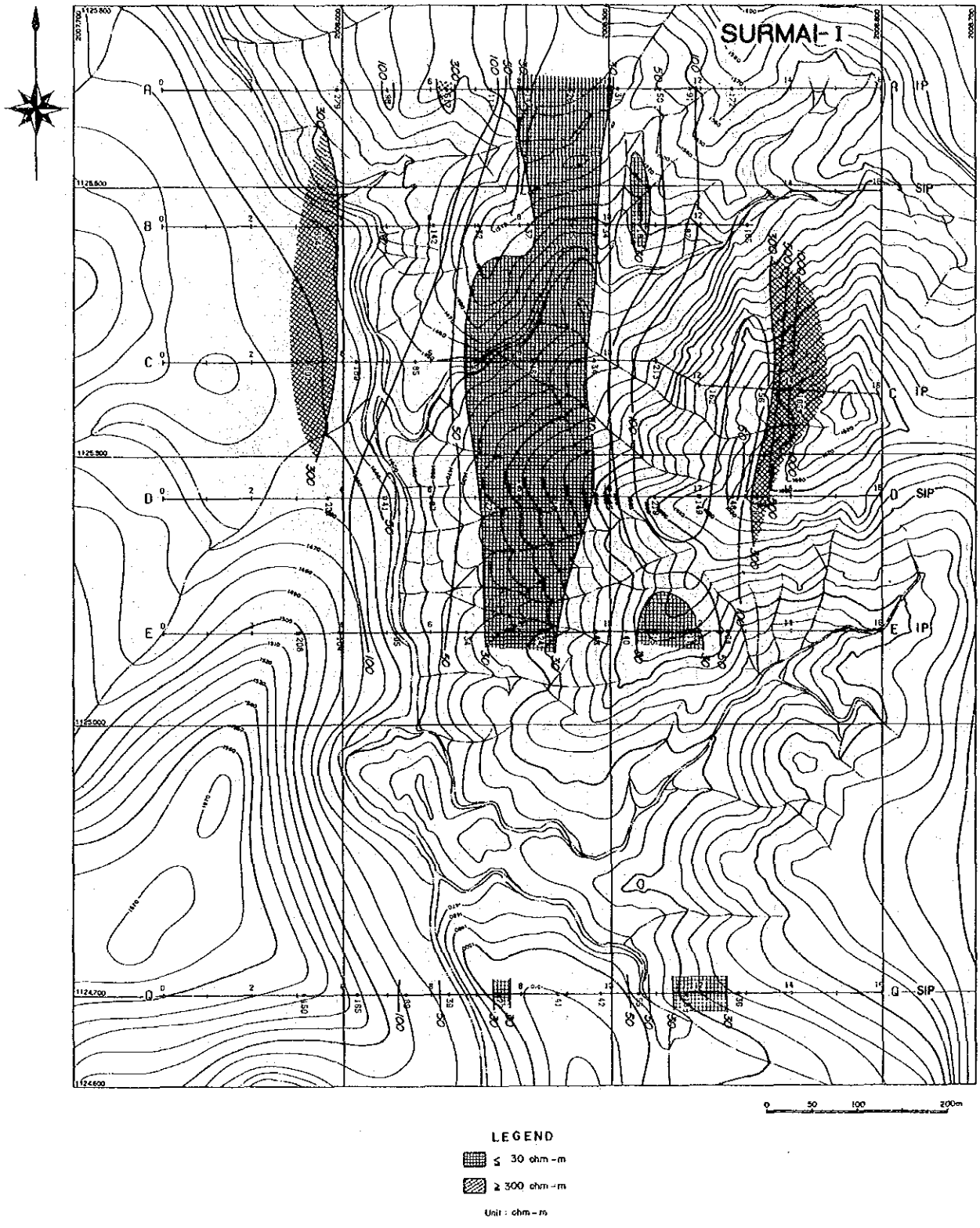

Fig. Ⅲ-3-12(3) Plan Map (n=5) of Apparent Resistivity in Surmai I Area

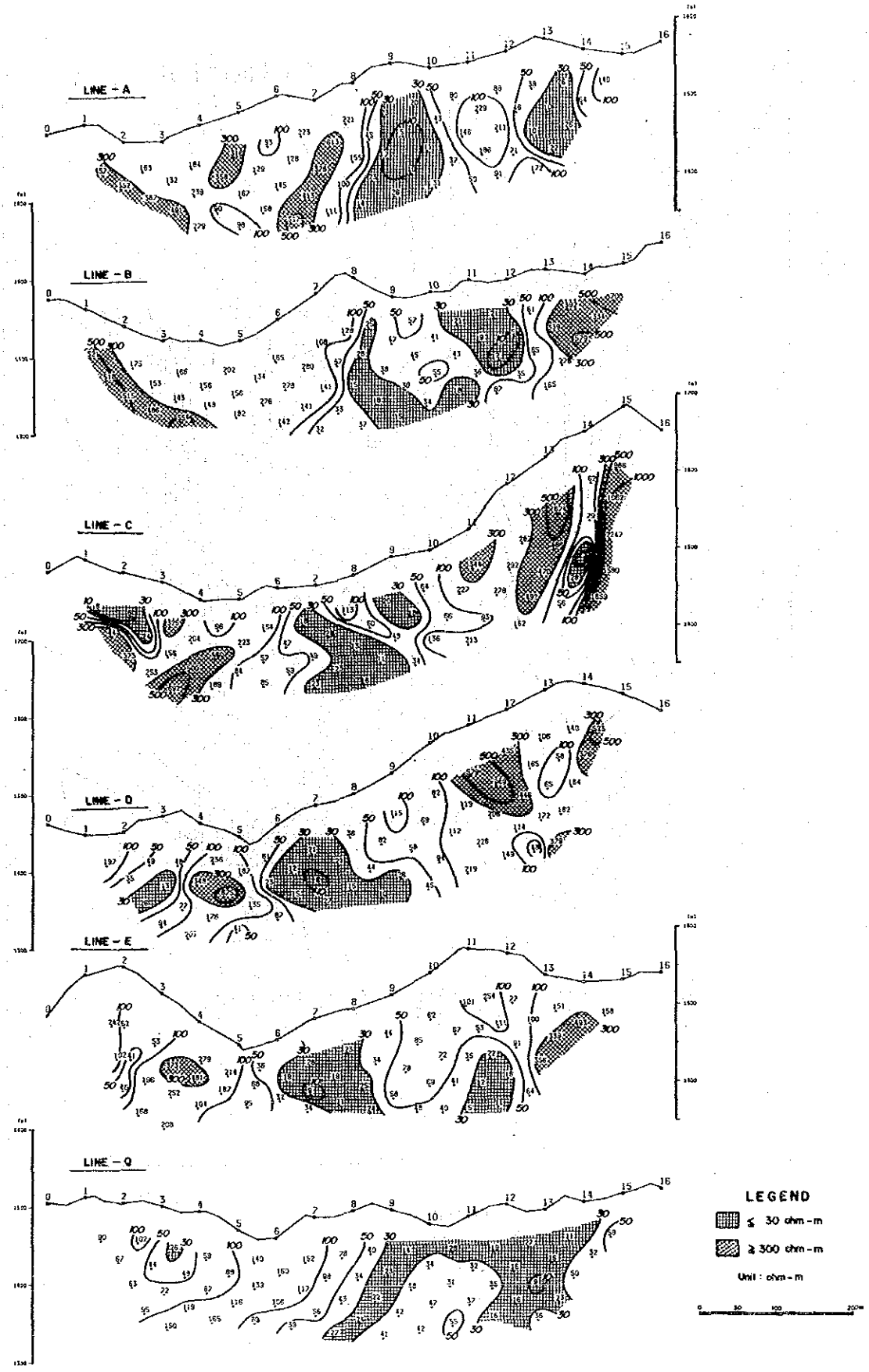

Fig. Ⅲ-3-13 Panel Diagram of Apparent Resistivity in Surmai I Area

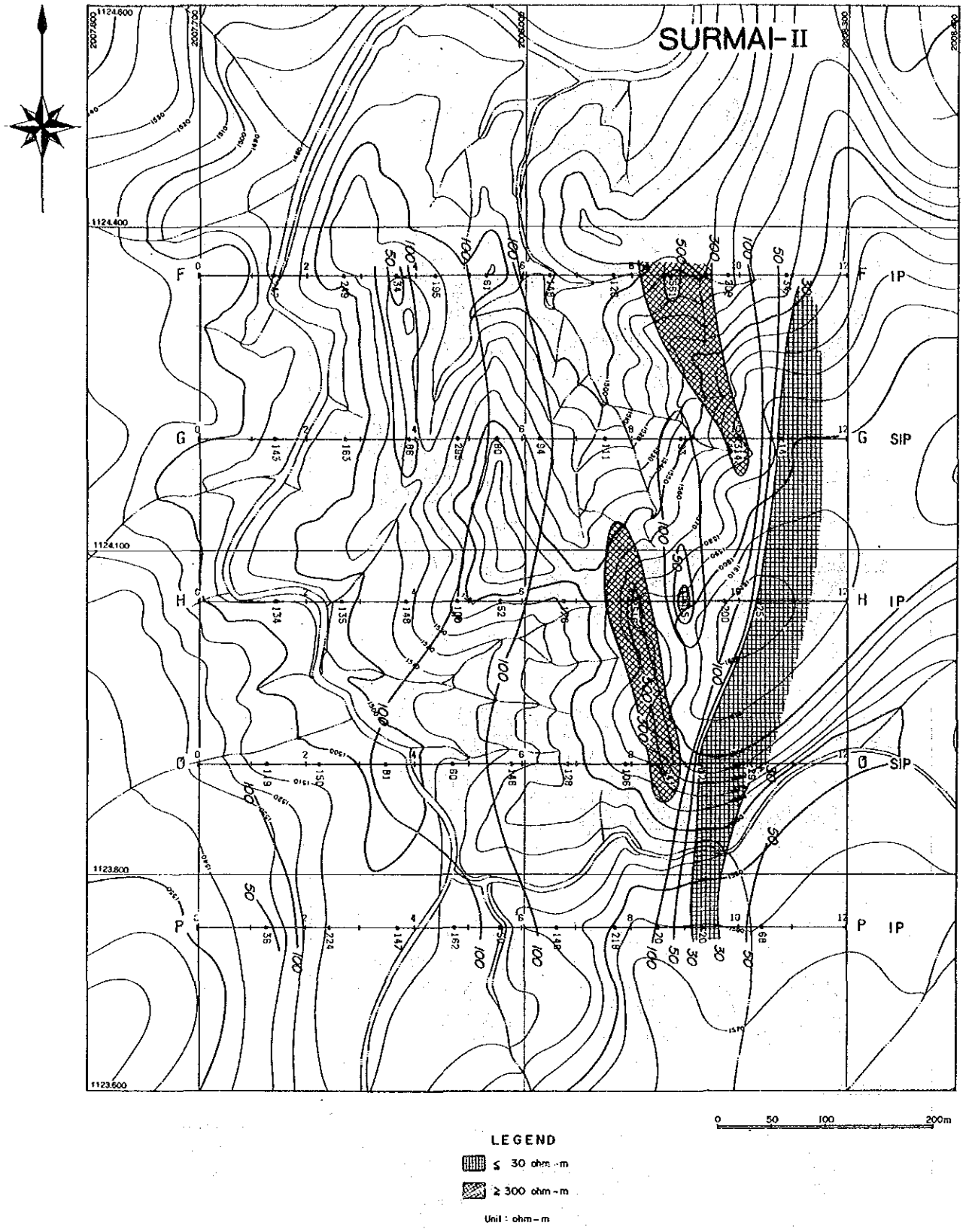

Fig. Ⅲ-3-14(1) Plan Map (n=1) of Apparent Resistivity in Surmai Ⅱ Area

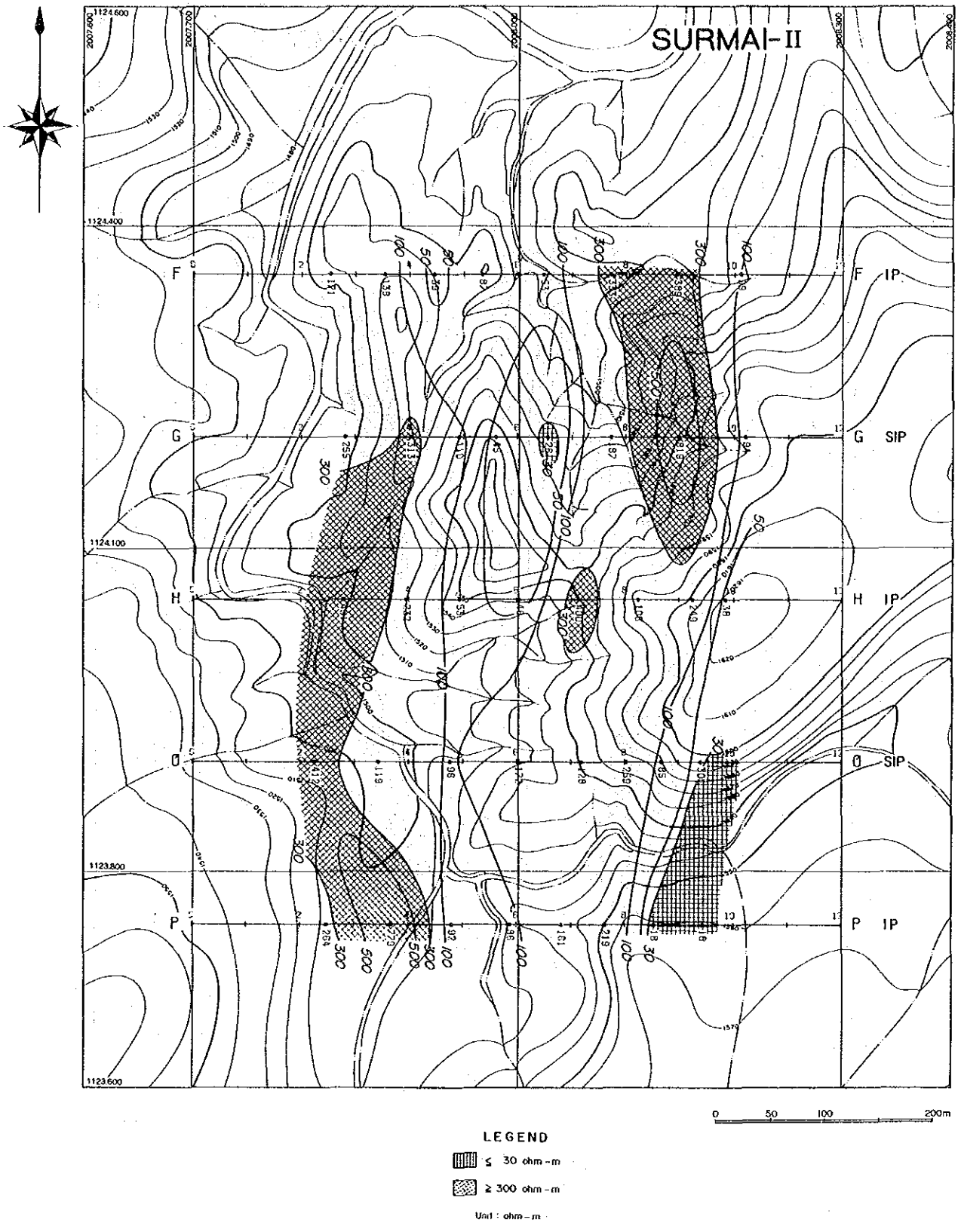

Fig. Ⅲ-3-14(2) Plan Map (n=3) of Apparent Resistivity in Surmai Ⅱ Area

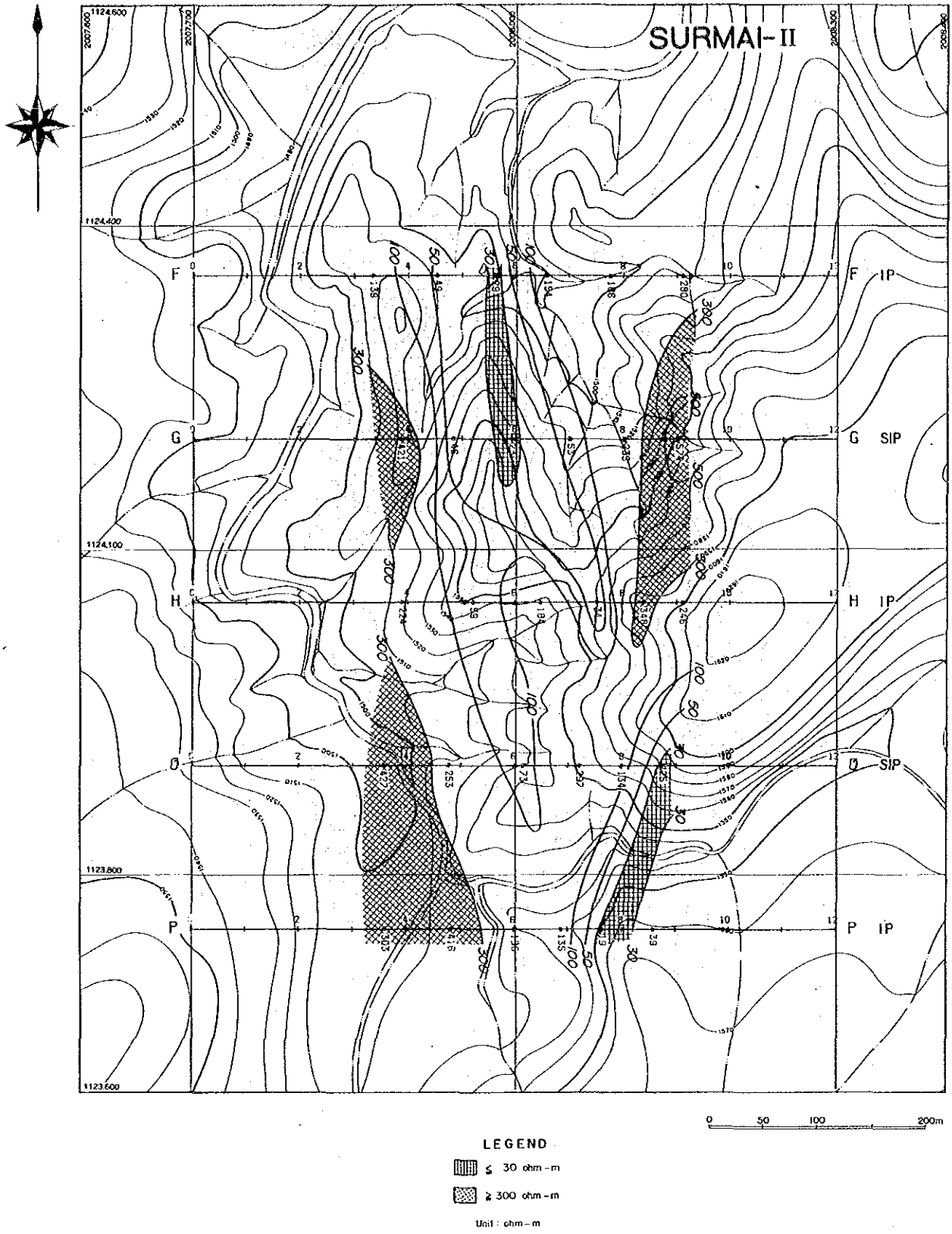

Fig. Ⅲ-3-14(3) Plan Map (n=5) of Apparent Resistivity in Surmai Ⅱ Area

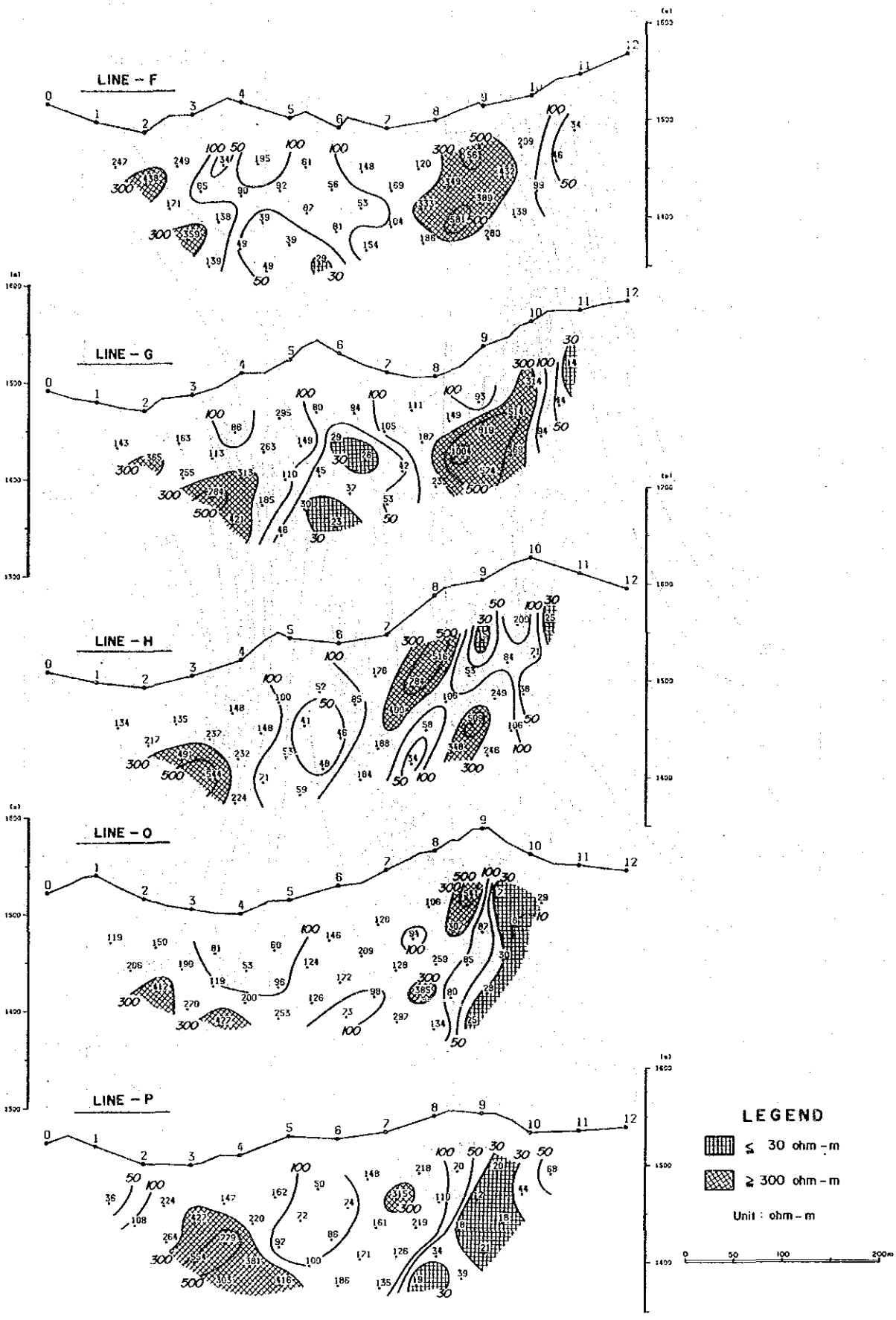

Fig. Ⅲ-3-15 Panel Diagrm of Apparent Resistivity in Surmai Ⅱ Area

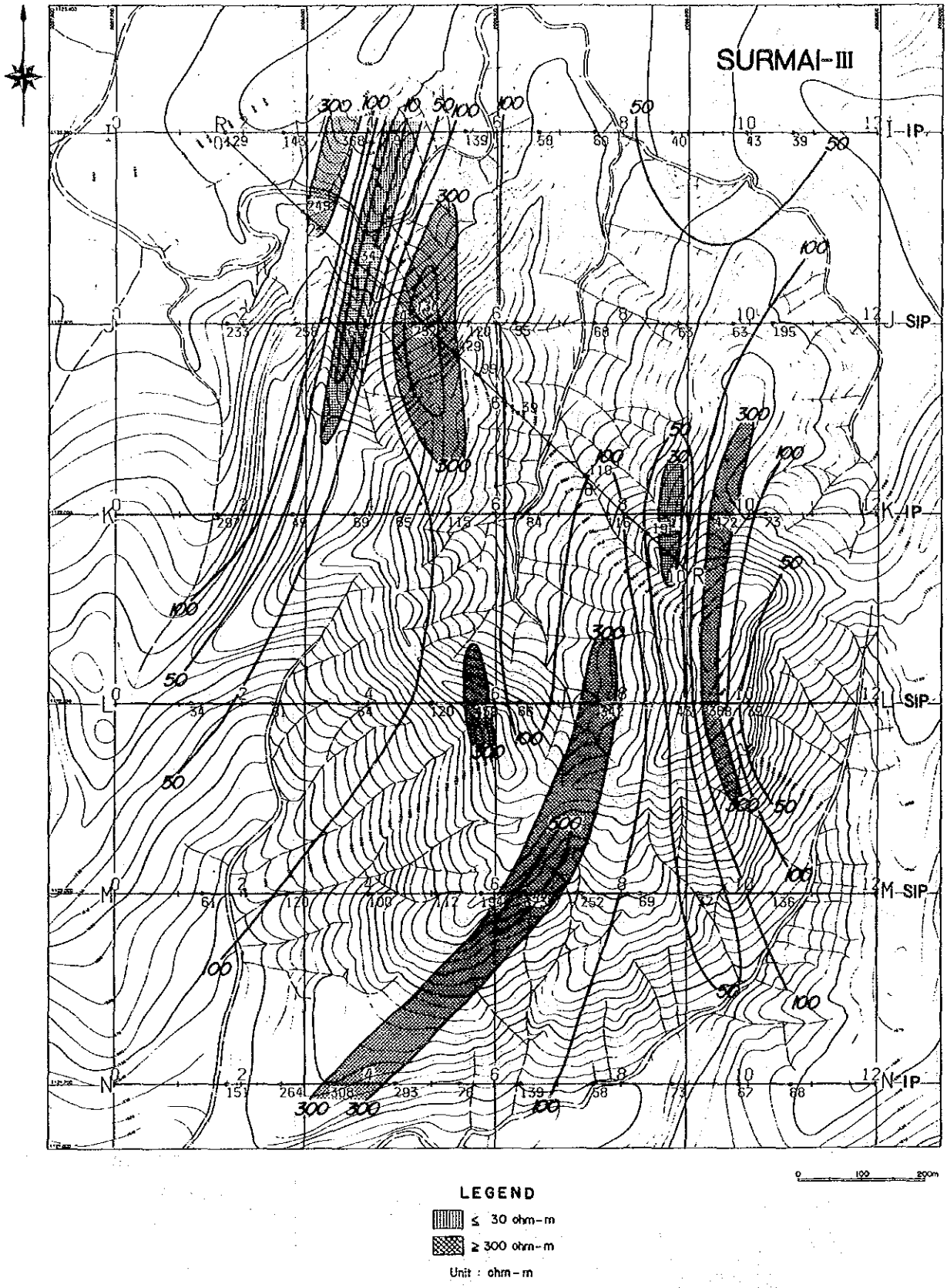

Fig. Ⅲ-3-16(1) Plan Map (n=1) of Apparent Resistivity in Surmai Ⅲ Area

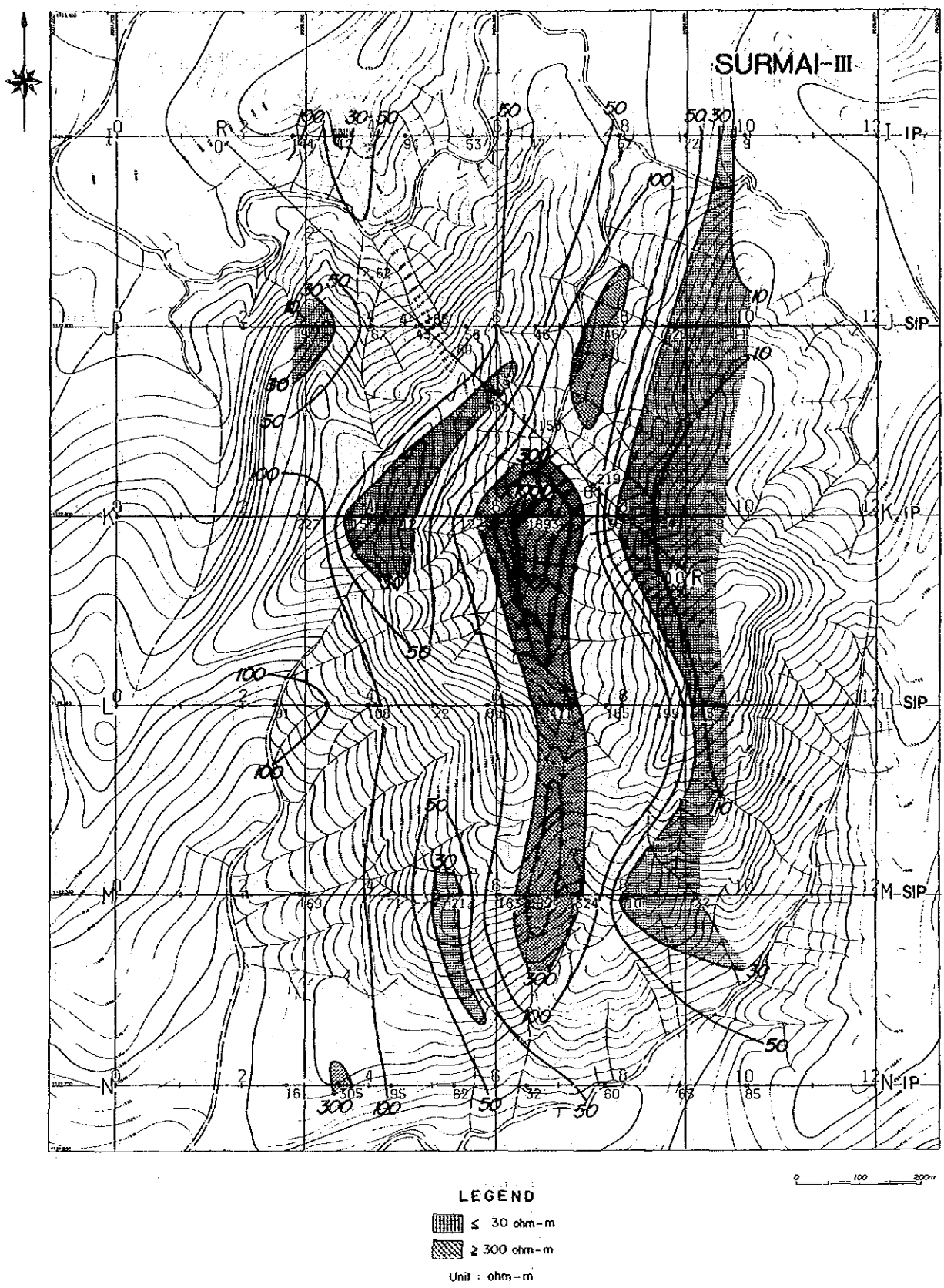

Fig. Ⅲ-3-16(2) Plan Map (n=3) of Apparent Resistivity in Surmai Ⅲ Area

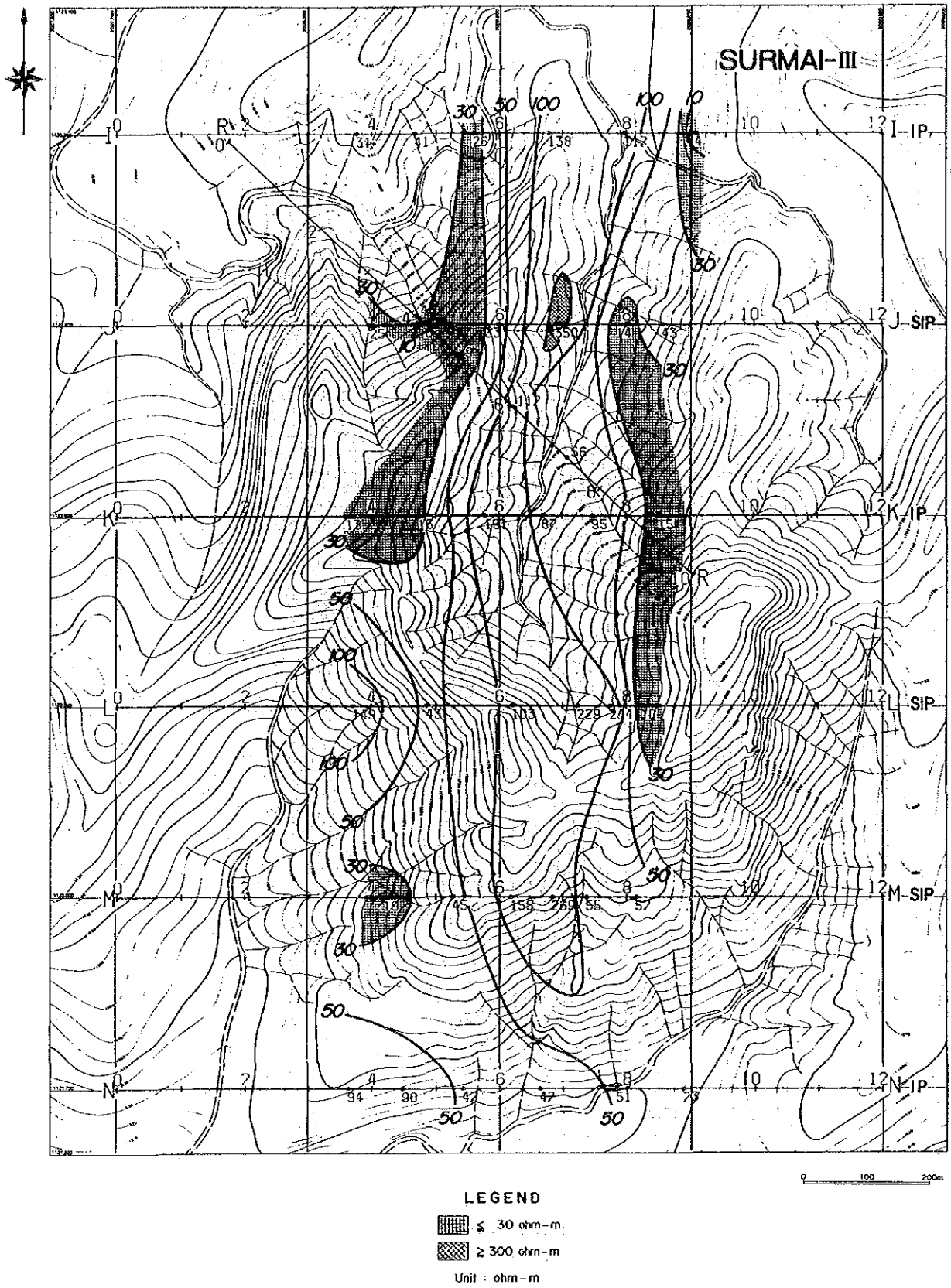

Fig. Ⅲ-3-16(3) Plan Map (n=5) of Apparent Resistivity in Surmai Ⅲ Area

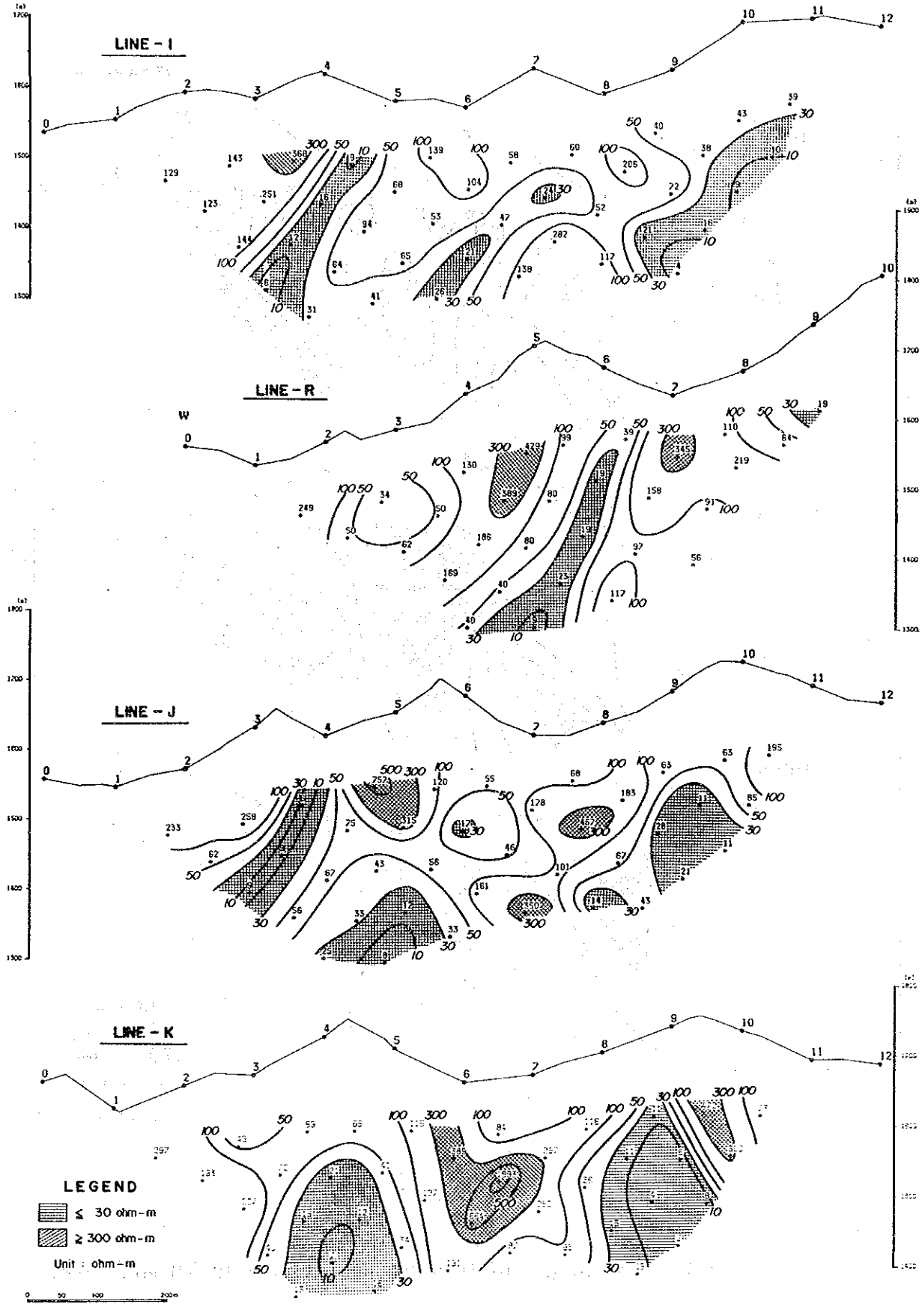

Fig. Ⅲ-3-17(1) Panel Diagrm of Apparent Resistivity in Surmai Ⅲ Area

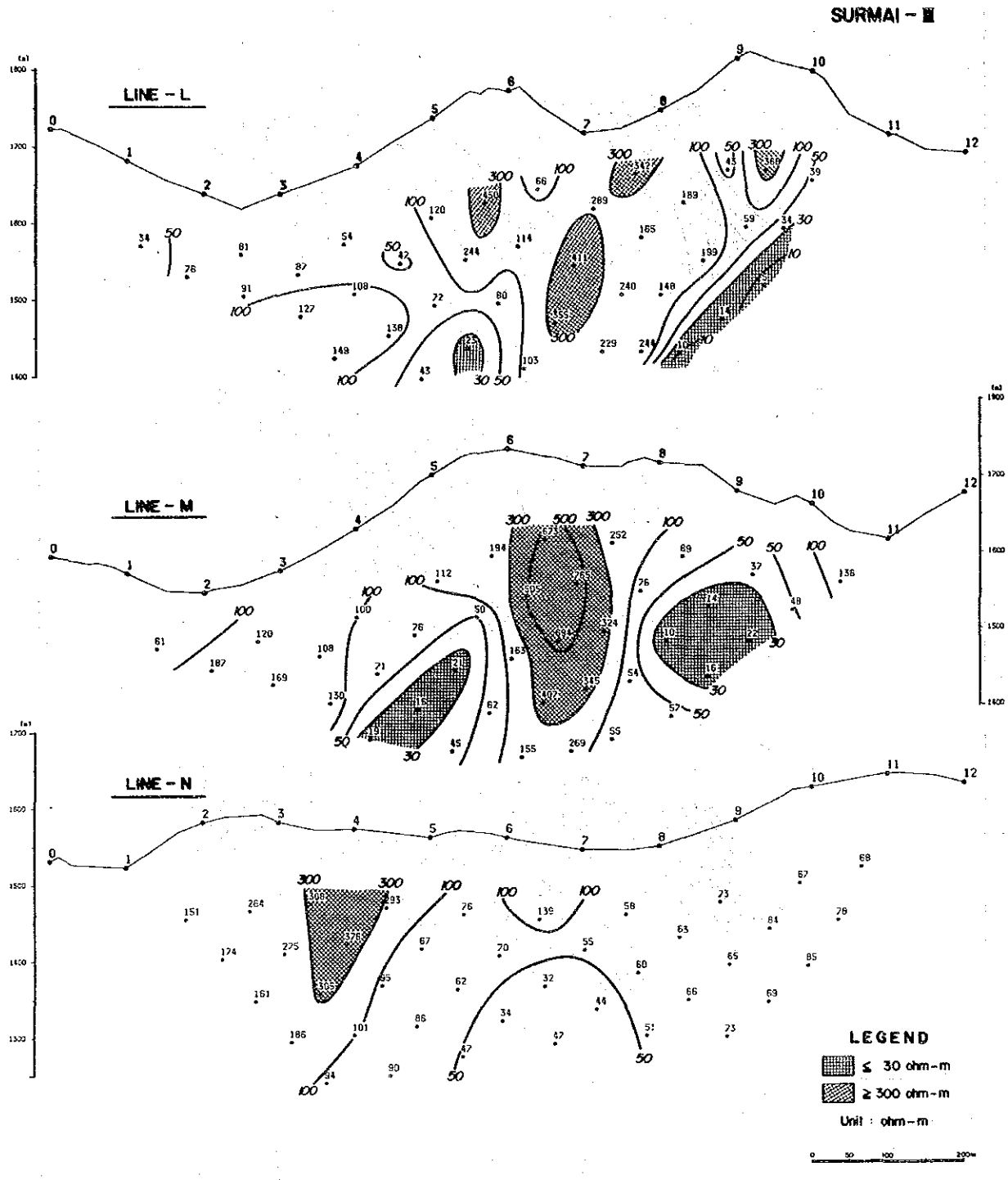

Fig. Ⅲ-3-17(2) Panel Diagrm of Apparent Resistivity in Surmai Ⅲ Area

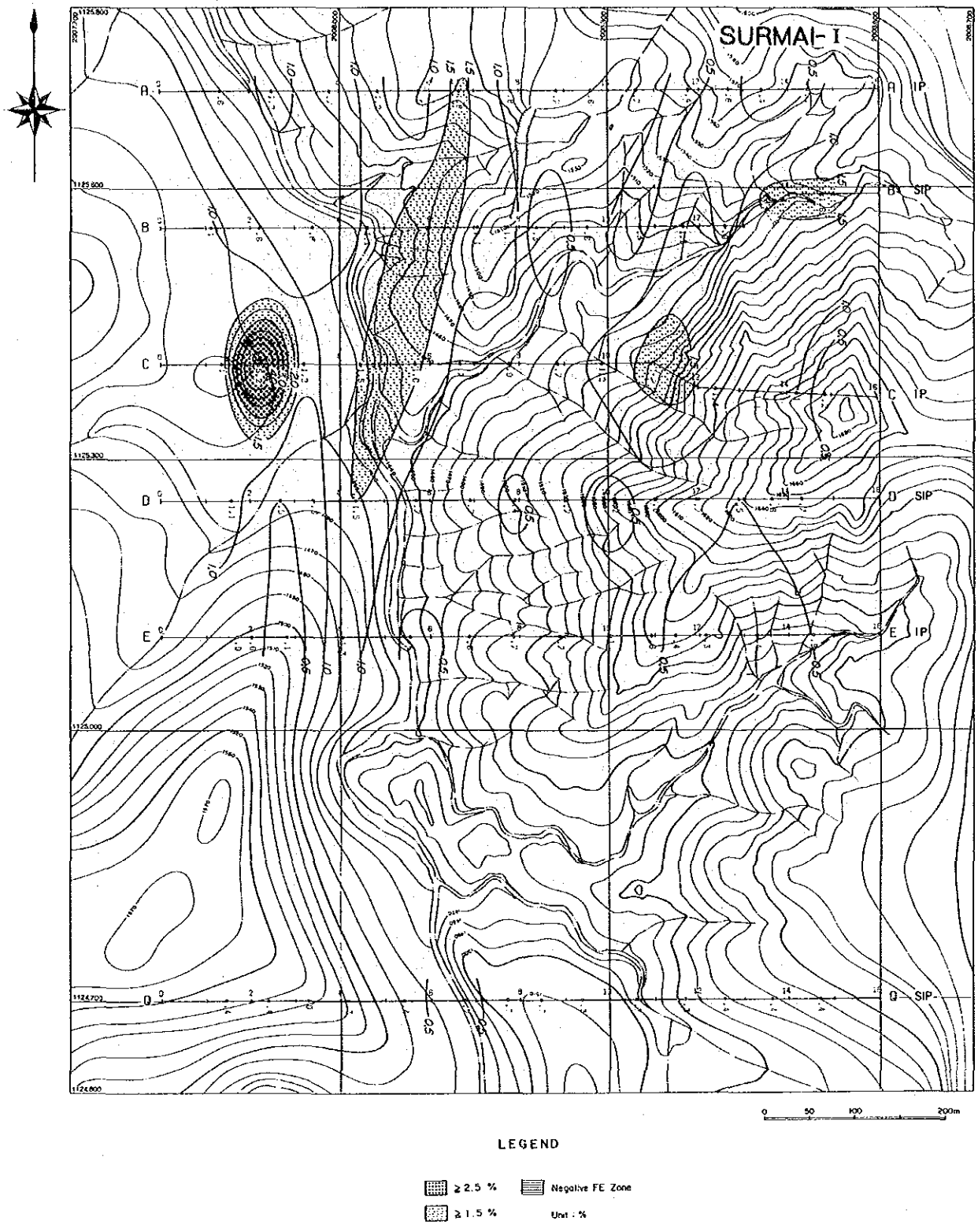

Fig. Ⅲ-3-18(1) Plan Map (n=1) of PFE in Surmai I Area

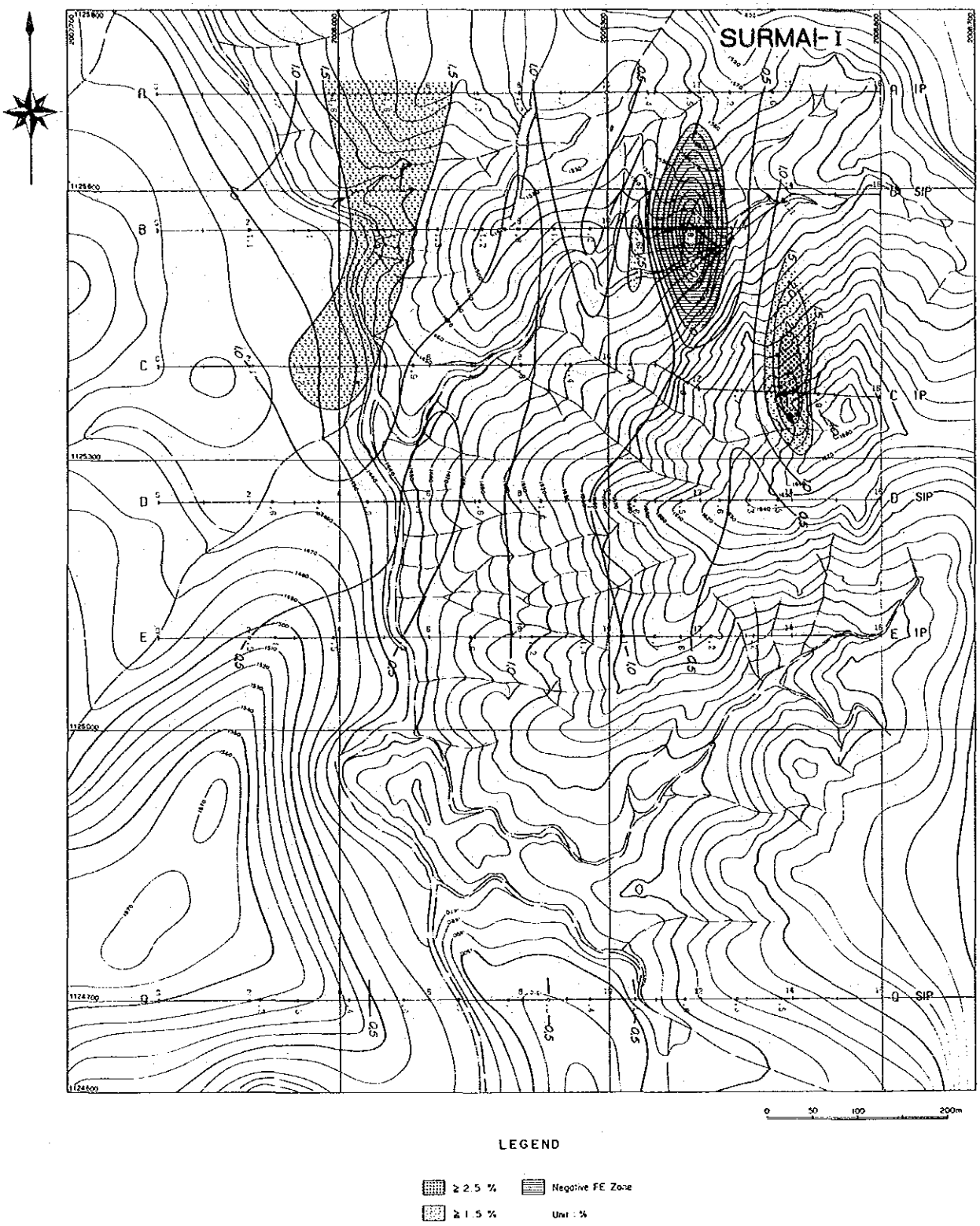

Fig. Ⅲ-3-18(2) Plan Map (n=3) of PFE in Surmai I Area